

## Article

# The Study of Electrical Energy Power Supply System for UAVs Based on the Energy Storage Technology

Khac Lam Pham <sup>1,\*</sup>, Jan Leuchter <sup>1</sup>, Radek Bystricky <sup>1</sup>, Milos Andrlé <sup>1</sup>, Ngoc Nam Pham <sup>2</sup>  
and Van Thuan Pham <sup>3</sup>

<sup>1</sup> Department of Aviation Technology, University of Defence, 662 10 Brno, Czech Republic

<sup>2</sup> Department of Microelectronics, Brno University of Technology, 616 00 Brno, Czech Republic

<sup>3</sup> Department of Air Defence, University of Defence, 662 10 Brno, Czech Republic

\* Correspondence: khaclam.pham@unob.cz

**Abstract:** Unmanned aerial vehicles (UAVs) are increasingly attracting investment and development attention from many countries all over the world due to their great advantages. However, one of the biggest challenges for researchers is the problem of supplying energy to UAVs to ensure they can operate for a longer time. Especially in the case of rotary wings, they consume more energy than other UAV types as the motors need to spend a lot of energy to operate in order to overcome the gravity of the earth. The article aims to research power supply, energy consumption on UAVs, and a method of taking advantage of external energy sources to provide power for the operation of UAVs and discuss UAVs' structure, categories, and control. Two experiments were conducted separately to evaluate the energy consumption of UAVs and the energy conversion from external energy sources to electrical energy. A test bench was designed to evaluate and determine the maximum efficiency using regenerative braking mode. The measuring device was manufactured to measure the necessary parameters to calculate the energy consumption and performance of the system. Experimental numerical results show that energy conversion from external sources is one of methods that can help increase the flight time of the UAV.

**Keywords:** energy consumption; unmanned aerial vehicle; quadrotor; efficiency



**Citation:** Pham, K.L.; Leuchter, J.; Bystricky, R.; Andrlé, M.; Pham, N.N.; Pham, V.T. The Study of Electrical Energy Power Supply System for UAVs Based on the Energy Storage Technology. *Aerospace* **2022**, *9*, 500. <https://doi.org/10.3390/aerospace9090500>

Academic Editor: Hailong Huang and Chao Huang

Received: 17 June 2022

Accepted: 30 August 2022

Published: 7 September 2022

**Publisher's Note:** MDPI stays neutral with regard to jurisdictional claims in published maps and institutional affiliations.



**Copyright:** © 2022 by the authors. Licensee MDPI, Basel, Switzerland. This article is an open access article distributed under the terms and conditions of the Creative Commons Attribution (CC BY) license (<https://creativecommons.org/licenses/by/4.0/>).

## 1. Introduction

Since their appearance in the early 19th century, unmanned aerial vehicles (UAVs) have been invested in research and development by many countries around the world. In the beginning, UAVs were used mainly in the military field and accounted for 90% of the UAV's market share. Nowadays, with the development of science and technology, UAVs have integrated various modules, such as sensors, cameras, and Lidar, making them more applicable in the civil field. Therefore, unmanned aerial vehicles (UAVs) are increasingly improved and have some advantages over traditional manned vehicles, such as compact size, cost of manufacturing, and maintenance. Along with that, recreational and industrial interests cause the UAV's market share to increase to more than 50% in the nonmilitary field. According to the latest data, the global market size of UAVs is predicted to be worth USD 32 billion in 2022 and could reach USD 72 billion by 2028 with a compound annual growth rate of 14.4% [1,2]. In the civil field, UAVs have a wide range of applications in agriculture, such as seed planting, weed recognition, insecticide and fertilizer prospecting and spraying [3,4], monitoring and data collection [5], delivery of goods [6], photography [7], mapping, and numerous other applications [8]. In addition, UAVs are increasingly used in the military field, such as reconnaissance, surveillance of enemy activity [9,10], radar system jamming, shadowing enemy fleets, decoying missiles, or executing attack missions [11]. Some applications of UAVs are shown in Figure 1.

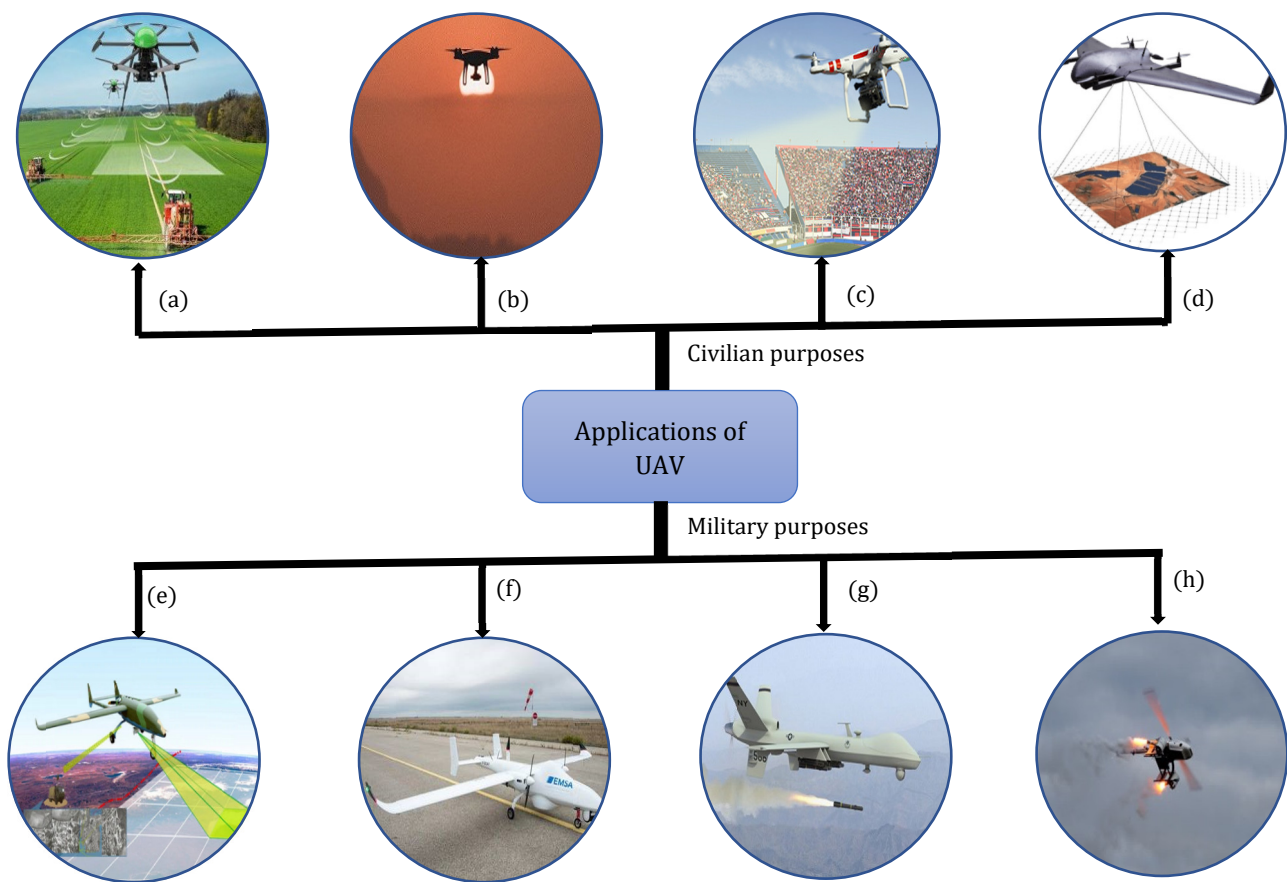


**Figure 1.** Applications of UAVs in: (a) agriculture [11], (b) monitoring and data collection (pollution and land monitoring) [12], (c) photography (film, video) [13], (d) aerial mapping [14], (e) reconnaissance [15], (f) surveillance of enemy activity [16], (g) attack missions [17], (h) decoying missiles by the emission of artificial signatures [18].

One of the most important tasks when designing and building a UAV is to make sure the system is operational for as long as possible, which means increasing the endurance of the UAV. There are many methods used to solve this problem, such as designing UAV shapes with optimal aerodynamic parameters to reduce friction and aerodynamic drag or reducing the system weight of the UAV [19–21]. These methods have many advantages, but when they reach a certain stage, it is difficult to advance further. Another approach that many researchers have focused their research on is to solve the problem of power supply for UAVs. The capacity limitation of a UAV energy storage system is a crucial technical challenge for UAV applications. Among UAV types, the multirotor is one of the fastest-power-consuming machines. Most of them have a battery life of less than 60 min [22–25]. To solve this problem, there are two options: increase the battery capacity and recharge the battery. However, in the case of increasing battery capacity, this option has a few disadvantages when the current battery technology is quite limited. Precisely, as the battery capacity increases, the mass of the battery that the UAV needs to carry will increase. Many methods have been studied to increase the energy density contained in the battery, but not much progress has been made yet. To increase the operating time of the UAV, the method of re-energizing the battery from external sources has been focused on research and development. There are two methods of charging the battery: wireless and wired charging. The current wired charging technique has limitations, such as complexity, insufficient mobility, and low efficiency. Meanwhile, the wireless charging technique has solved the limitations of wired charging when it provides sufficiently greater freedom of movement. UAVs can operate for longer periods of time and continuously without the

need to return to their base for charging. There are a wide range of wireless charging methods that have been researched and developed to find an efficient battery charging technique. These methods have their own advantages and disadvantages. In addition, they will be discussed in more detail later in the paper.

This paper focuses on the recharging technique using wind power to convert mechanical energy into electrical energy to improve the endurance of UAVs and the capacity of the electrical energy power supply system for UAVs. When the UAV flies to a certain height, taking advantage of the wind as the UAV descends, the wind causes a force on the propeller, causing the motor to rotate using windmilling, which will generate electrical energy and charge back the battery or supercapacitor on the UAV. In this paper, we will discuss the energy storage technology and power supply for electric UAVs to improve the flight time and possibilities of wireless charging techniques for UAVs.

## 2. Concept of an Electric UAV

### 2.1. Brief Description of UAVs

Currently, UAVs have many types and are used in various fields, from civil to military. Therefore, many criteria have been proposed to classify UAVs into different groups, such as endurance, flight range, flying mode, size, mission, and application. In [26], they are divided into five groups according to operations: unmanned ground vehicles, unmanned aerial vehicles, unmanned surface vehicles, unmanned underwater vehicles, and unmanned spacecraft. Authors in [27] classify UAVs into three categories based on robotics: autonomous, shared autonomous, and teleoperation systems. Based on aerodynamic configuration, UAVs can be divided into three categories: fixed wing, rotary wing, and flapping wing. The advantages and disadvantages of these UAVs are shown in Table 1.

**Table 1.** Comparison between UAV types [27].

UAV Types	Cost	Maneuver	Construction and Repairing	Range	Flight Safety	Energy Consumption	Civilian Application	Military Application
Rotary wing	Medium	High	Medium	Medium	Medium	High	High	Medium
Fixed wing	Medium	Low	Medium	High	Medium	Low	Medium	High
Flapping wing	High	Medium	High	Low	Low	Medium	Medium	Low

From Table 1, it can be seen that the rotary-wing UAV (multirotor) is used more commonly in both civil and military applications due to advantages, such as cost and high maneuverability. In 2004, most UAVs were produced for military purposes. UAVs intended for civilian use accounted for a very small and insignificant proportion compared with 98% of UAVs used in the military [28]. At that time, fixed-wing UAVs were most commonly used in the military field. With the development and popularity of science and technology available on UAVs to hobbyists, rotary-wing UAVs are increasingly interesting to hobbyists, commercial organizations, and governments. Rotary-wing UAVs account for 62.8% of the global market share, while fixed-wing and the rest account for 25.4% and 12%, respectively [29]. However, the problem of energy consumption of rotary-wing UAVs is still a big challenge when it consumes higher energy compared with the other two types. Rotary-wing UAVs often use many motors to help the UAV overcome the gravity of the earth, so the energy consumed for it is very large, making the flight time of the rotary wing shorter. In addition, commercial rotary-wing UAVs usually have a flight time of less than 1 h. Therefore, in this paper, the authors focus on solutions to solve the problem of power supply for rotary-wing systems (especially, quadrotors). However, before moving forward with that, let us first briefly discuss the UAV's components.

The UAV system is made up of many different components. Depending on the requirements of the mission, parts of the UAV may be changed. However, they basically include

the following subsystems: navigation, air vehicle, payload, communications, launch, recovery and retrieval equipment, and control station. These subsystems do not exist in isolation but are parts of a total system. The structure of the UAV can be seen in Figure 2.

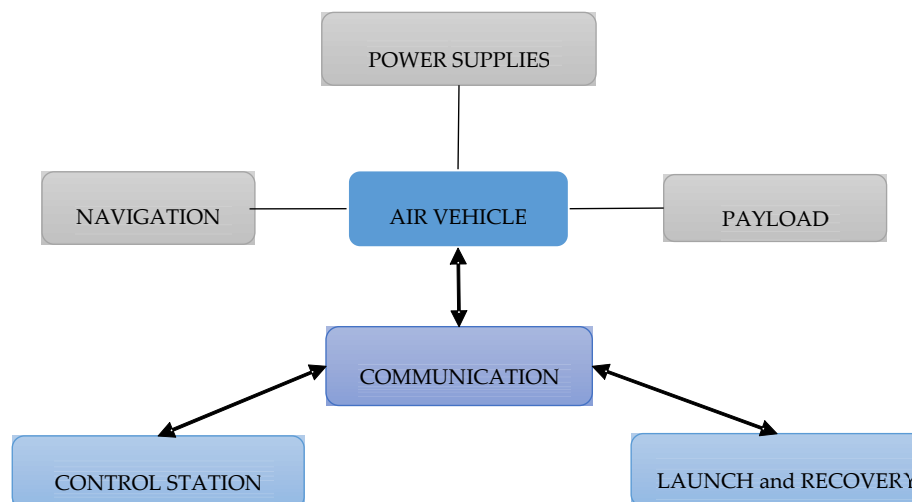


**Figure 2.** Functional structure of an UAV.

*Air vehicle* (aircraft) is used to carry subsystems for it to operate, such as communications link, control equipment, power plant, and fuel. In addition, aircraft carry the mission payload to its point of application. Air vehicles are designed and manufactured mainly based on the need for operational missions. The factors that can affect an aircraft's design are drag, lifting forces, thrust generated, and gravity. *Payload*, based on the need for operational tasks, the type, and the performance of the payload, can be different. However, it basically can be divided into two types: video cameras, thermal imaging cameras, sensors [17], and loads, such as weapons, missiles, and bombs for the military, and crop spray fluid, firefighting materials for civil purposes, and so on [18]. When designing a UAV, the payload is one of the important factors to consider. A heavier payload will affect the energy required for the UAV to operate. This leads to a trade-off in the flight duration of the UAV. *Launch, recovery, and retrieval equipment*, Launch equipment is used on those air vehicles that do not have the capability of vertical flight. The equipment could be in the form of a ramp, propelled by a system of compressed air and so on. Recovery equipment is also needed for air vehicles without vertical flight capability. The recovery equipment could be a parachute installed within the air vehicle, a large net, or a carousel apparatus. Retrieval equipment is required to transport the UAV back to its launcher. A *communication system* is required to provide a link between the control station and the air vehicle. Communication can be achieved by three methods: radio, fiber optics, and laser beam. However, the transmissions widely used are at radio frequencies. *The control station* (CS) is the center of the operation and the man–machine interface. Via a communication system, from the control station, the operator can send control commands to the aircraft so the UAV can perform various tasks. In addition, at the CS, the operator can get information from sensors, cameras, other payloads, position, and status information of the UAV [30,31].

In this paper, our aim is to accumulate energy from an external power source to improve the endurance of the UAV. By knowing the trajectory of the UAV, it is possible to calculate the energy consumed for the flight. In addition, a navigation system is an important factor needed to be able to calculate the trajectory of the UAV. *The navigation system* is necessary for the operator to know the position and status of the UAV to control it during flight.

In the past, an expensive, complex, and sophisticated system called INS (inertial navigation system) was used for navigation. However, it required frequent positional updates from the control station using radio tracking or recognition of geographical features.

Since the appearance of the global navigation satellite system (GNSS), the UAV can access positional information in real time, which helps to ease this problem. The GNSSs now available are compact, light, and quite cheap. The GNSS currently has four systems used in the world: GPS, GLONASS, Galileo, and BeiDou. GPS (Global Positioning System) provides a Precise Positioning Service (PPS) for authorized users with P(Y) and M signals at the frequencies L1 (1575, 42 MHz) and L2 (1227, 60 MHz) and Standard Positioning Service (SPS) for others. GLONASS consists of 24 satellites of the Uragan-M block, which have been launched since 2001 and which provide the SF (Obfuscated FDMA) service to authorized users and the OF service to other users. Unlike other GNSSs that use the CDMA (Code Division Multiple Access) method, GLONASS uses the FDMA (Frequency Division Multiple Access) method. As regards Galileo, from a planned number of 30 satellites, 26 have been launched so far, and 4 satellites are not in use. One pair of satellites did not achieve proper orbit due to carrier failure, another had very low power, and 1 failed a flight clock. The BeiDou system (BDS) is operated in two variants: the older BDS-2 has been fully functional since 2012, and the newer BDS-3 since 2020. By connecting these satellites and knowing their positions, it is possible to calculate the coordinates and the speed and altitude of the UAV. Using these parameters from the calculation of GNSS data can help to plan the trajectory of the UAV, and it can be useful for power management using energy storage technologies.

Figure 3 shows a UAV flight scenario. During the flight from the starting point to the ending point, the UAV consumes a lot of energy in the C1 and C2 areas and stores the energy back by converting wind energy into electric energy in R1 area. In order to achieve the goal of generating the maximum of the UAV coefficient of efficiency, it is necessary to find the efficient coefficient of wind energy to electric energy conversion. Since the UAV is affected by environmental factors and the variable speed of the motors, the power consumption model of the UAV is in fact a nonlinear model. The energy consumption model will become complex due to many parameters to be considered. However, our aim is to find the maximum efficiency; therefore, in this paper, the energy consumption model will be considered in linear form.

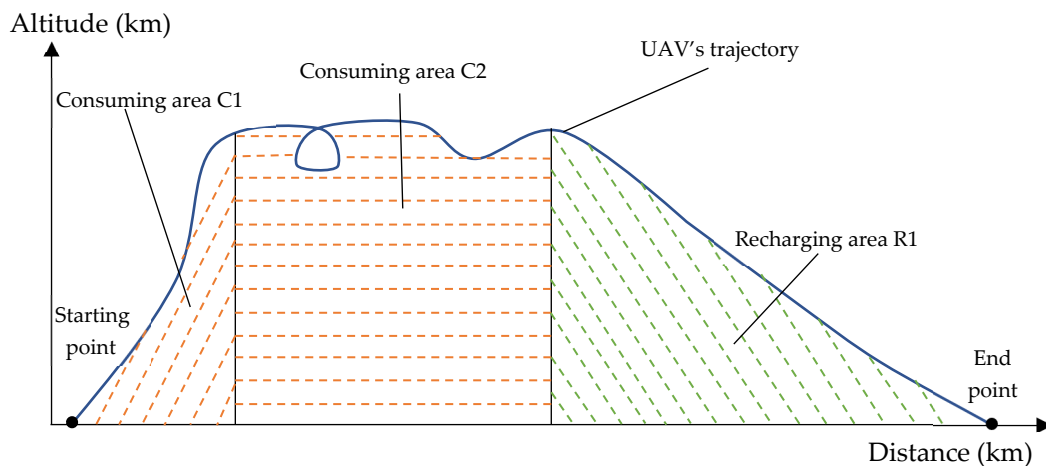


**Figure 3.** UAV flight scenario to get maximum efficiency.

The UAV's energy consumption is mainly concentrated in the propulsion system. The current flowing through the motor is very large, so the quadrotor usually has a short operating time. The propulsion power consumption can be calculated as

$$E_{pr} = \int_{t_0}^{t_f} \sum_{i=1}^4 \left( J\dot{\omega}_i(t) + K_T\omega_i^2(t) + D_v\omega_i(t) \right) \omega_i(t) dt \quad (1)$$

where  $\omega_i$  is the angular velocity of motor  $i$ ,  $J$  is the inertia of the motor,  $D_v$  is the viscous damping coefficient, and  $K_T$  is the drag coefficient.

The energy converted from wind energy can be calculated according to the following formula:

$$E_c = \int_{t_1}^{t_2} \eta_0 P_w(t) dt \quad (2)$$

where  $\eta_0$  is the efficiency coefficient of wind energy to electric energy conversion, and  $P_w$  is wind energy.

The UAV's performance between energy conversion and energy consumption can be calculated as follows:

$$\eta = \frac{E_c}{E_{pr}} \quad (3)$$

From Equations (1) and (2), it can be seen that the energy consumption of the UAV depends greatly on the angular velocity of the motors. It is very important to control the current of the electric motors or the electric drive of the system. The efficiency of these electric drives is affected by the level of the current. Meanwhile, energy conversion is affected by  $\eta_0$  and the wind energy through the cross section of the propeller. Therefore, in the following sections, we focus on discussing the concept of the electric drives of UAVs according to the technology of the energy storage elements, such as supercapacitors, batteries, and fuel cells.

## 2.2. Electric and Hybrid UAV Using Energy Storage Technologies

Aviation emits 2% of CO<sub>2</sub> annually and is predicted to increase to an average of 4% to 5% in the future. If this continues without taking concrete action to control it, ICAO expects emissions to roughly triple by 2050, which will account 25% of the global carbon emissions. Nowadays, the aviation industry can reduce noise and emission levels with the help of technological developments. Climate change concerns have led the aviation industry to explore more electric and hybrid electric propulsions as a potential path for reduced emissions during the last few decades [32].

**Parallel hybrid** (shown in Figure 4). These systems add the thrust or power generated by the ICE and the EM to propel the aircraft. The parallel hybrid has some advantages, such as high energy efficiency in steady conditions, low fuel consumption, and great synergy with nonhomogenous distributed propulsion. The drawbacks of a parallel hybrid are complex powertrain controllers and high complexity of distributed propulsion implementation, and in some cases, a mechanical coupler is needed.



Figure 4. Parallel hybrid [32].

**Serial hybrid** (shown in Figure 5). In these systems, the electric motor (EM) provides the entire power or thrust required. The ICE provides power to the electric propulsion system as a motor-generator. The pros of the serial hybrid are simplicity of powertrain control, good performance at low flight speed, and great synergy with distributed propulsion. They also have some disadvantages, such as high fuel consumption and energy losses as the ice mechanical energy is transformed into electric energy.

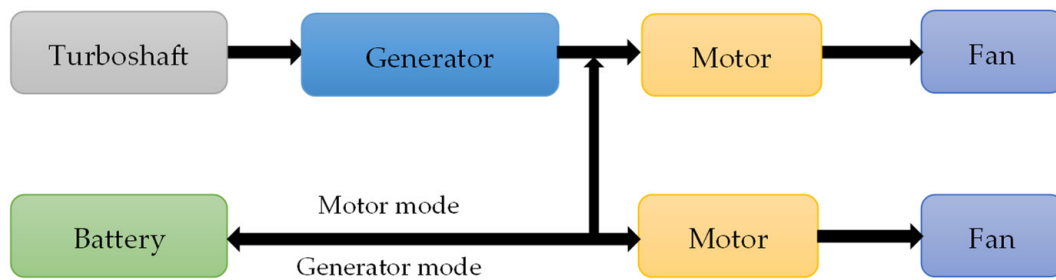


Figure 5. Serial hybrid [32].

**All electric** (shown in Figure 6). An all-electric propulsion system is widely used on small UAVs due to its advantages over other types. One advantage is having low noise. Electric motors make less noise when operating than fuel-powered engines. In addition, the all-electric propulsion system allows for a distributed use of smaller, quieter engines. Efficiency is also one of its advantages. The electric drive of the propulsion system can have more than 90% efficiency in comparison with 55% for large turbofans and 35% for small turbofans. Another advantage of all-electric propulsion systems is scalability. Precisely, the performance is the same when using one or two large motors or many small motors in electric propulsion systems. Therefore, in this paper, the research study focuses mainly on all-electric architecture using small UAVs. However, the energy problem of all-electric propulsion systems is the biggest challenge in designing UAVs [33].



Figure 6. All electric [32].

### Energy Management Strategy for UAVs

There have been many energy management strategies (EMSs) for UAVs studied and reported in various articles. The authors in [34] presented various EMSs for UAVs in different flight segments with varying sizes of battery packs. In [35], Xie et al., introduced a comprehensive review of conceptual design and energy management methodologies for hybrid electric-powered aircraft. In [36] Antonio Russo and Alberto Cavallo presented a method to deal with the stability analysis and the control of a supercapacitor based on the Second-Order Sliding Mode for a More Electric Aircraft. In [37], Giacomo et al., introduced an alternative EMS for aeronautic applications. The strategy is charging a battery in a nominal condition, and when the overload happens, the battery is used to help the generator.

Hybrid systems combine the advantages of different energy sources and balance their limitations, resulting in a significant increase in system performance. It is therefore very suitable for use in powering UAV systems. In EMS, power needs to be optimally split between power sources to achieve high performance of the system and efficiency of energy usage. The EMS can be mainly considered as follows: rule based, intelligent based, optimization based, and others (shown in Figure 7).

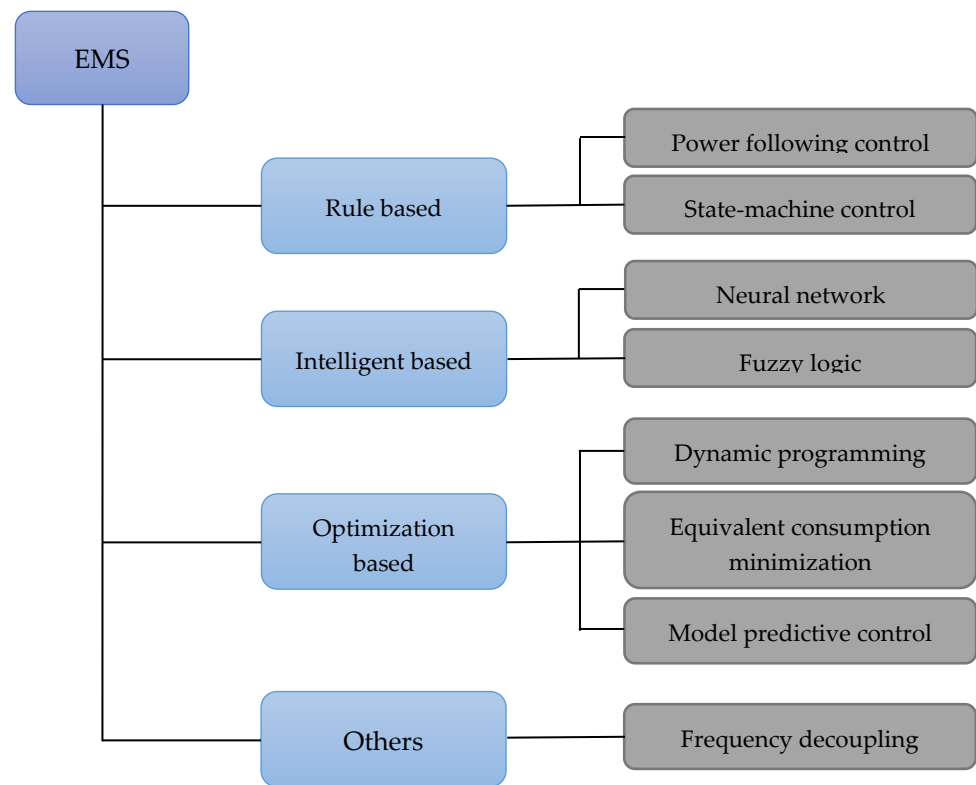


Figure 7. EMS classification for UAVs.

The architecture of an electric propulsion system can be seen in Figure 8. The Power management system controller will control the DC/DC converters so that the whole system can be supplied with the appropriate voltage to perform the task with high efficiency. In addition, the controller can prevent the system from overheating, overshooting, and overdischarging by monitoring the working state of the UAV.

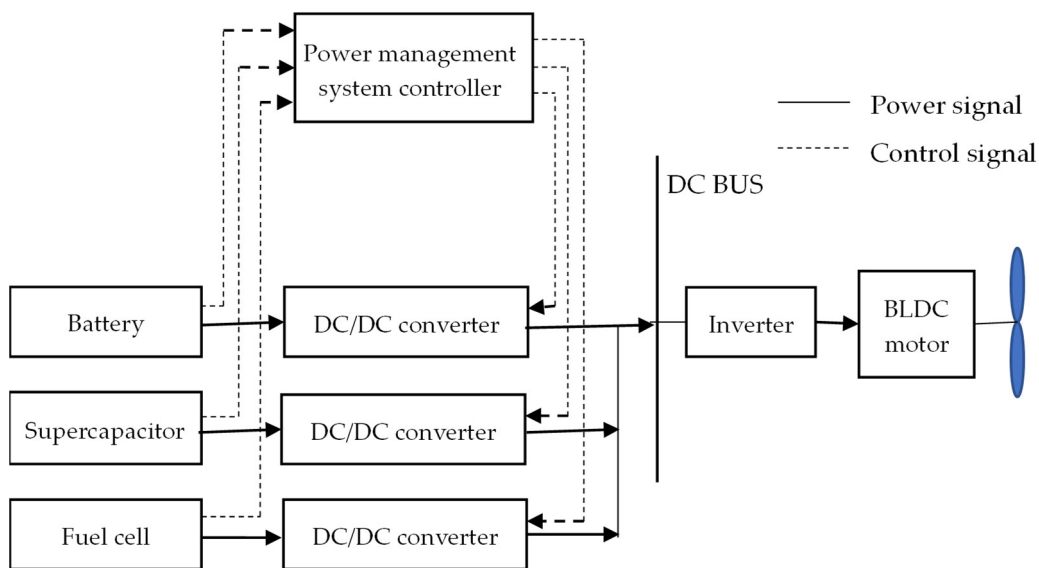


Figure 8. An architecture of an electric propulsion system on the hybrid system [34].

### 2.3. Power Sources Used in a UAV

The power system plays an important role in the UAV and is seen as the heart of the system as it supplies power for the whole operating system. The power system has

a significant effect on the flight performance of an aircraft. The power sources for UAV operation mainly include heat engine, fuel cell, supercapacitor, battery, and external energy source (solar, wind, etc.). They are divided into two categories: chemical system and electrical approaches (shown in Figure 9).

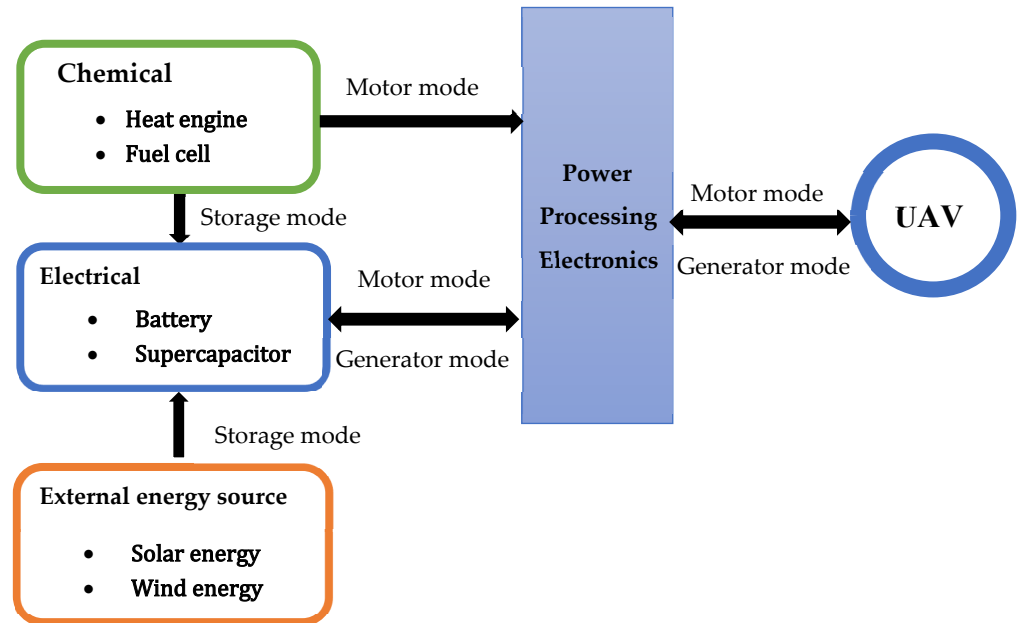


Figure 9. Power supplies in a UAV.

A heat engine is mainly used in large UAVs, such as HALE and MALE. It converts thermal energy into mechanical energy, which is the source of a UAV’s operation. However, because of complex control, high thermal signature, loud noise, low fuel economy, and the need for an auxiliary starting motor, a heat engine is not suitable for use in small UAVs.

Fuel cells (see Figure 10a) are used to convert the chemical energy of fuel into electricity. Hydrogen and oxygen are most commonly used as working substances for fuel cells in UAVs. The UAV using fuel cells as a power source usually has higher endurance as a fuel cell has five times higher energy density than a LiPo battery (see Figure 10). Nowadays, concerns about the lack of fossil fuel supplies and greenhouse gas emissions have led scientists to gradually reduce their interest in chemical energy sources and look for other green and cleaner energy sources.

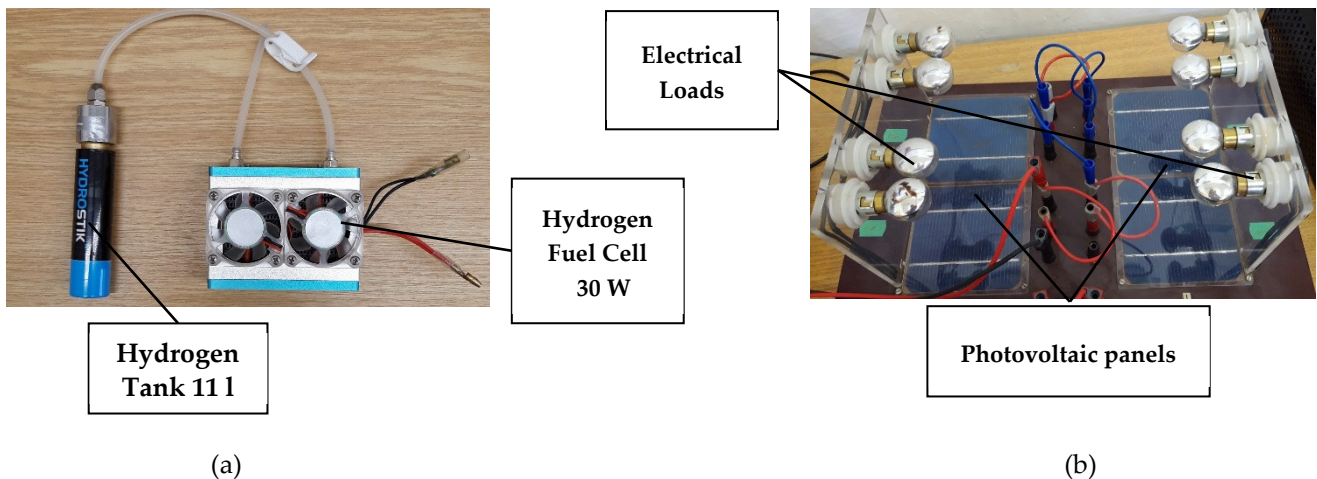
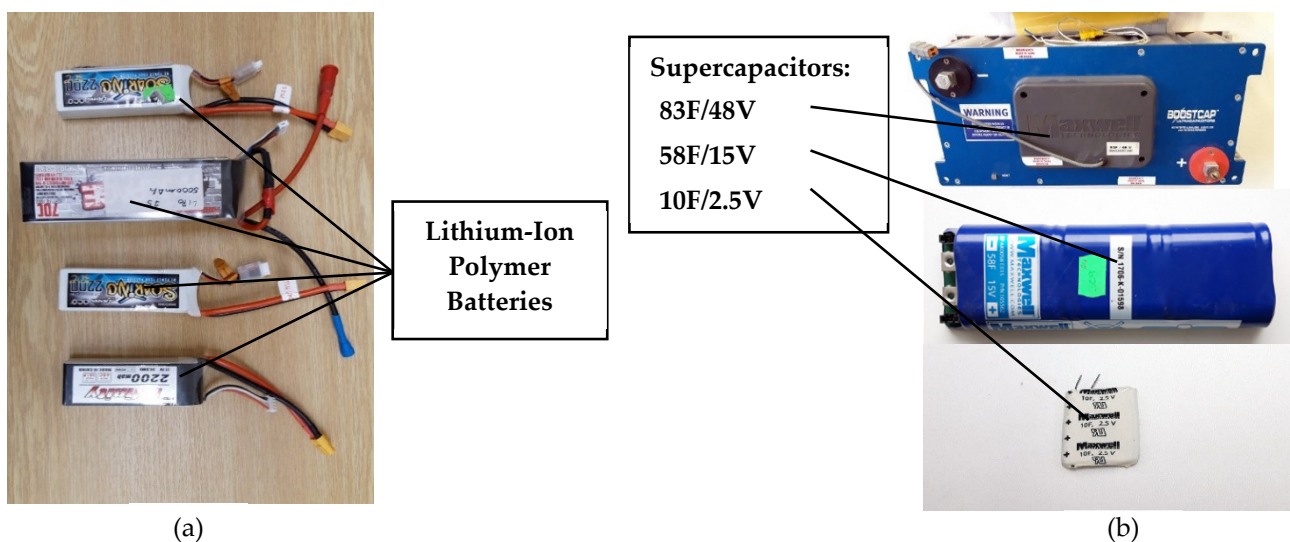


Figure 10. (a) Fuel cell; (b) solar power.

Electrical power has many advantages, such as reliability, no pollutant emission, high efficiency, low noise, self-starting feature, and a well-developed control system. Among the sources of electrical energy used on the UAV, the battery (Figure 11a) is the most commonly used one to power the system due to its cost-effectiveness, simplicity, and flexibility. However, batteries still have some limitations, such as low energy density and a long time to charge. In addition, in some cases of requiring a fast power response for the UAV's maneuver, the battery is not a good choice due to its slow power dynamic. To compensate for these drawbacks of the battery, using supercapacitors (see Figure 11b) could be considered when it has much higher power and can be a faster energy storage system (faster charge/discharge rate) compared with a battery. A supercapacitor also has a reasonable cost, a large operating temperature range, and a low maintenance cost and reduces the DC bus voltage fluctuation. However, in comparison with batteries, supercapacitors have lower specific energy capacities (only a few Wh/kg). Among supercapacitors, electrical double-layer capacitors are the most common types, which are very durable and capable of fast charging and discharging and have millions of cycles.



**Figure 11.** Electrical energy storage systems: (a) battery; (b) supercapacitors.

In Figure 12, it can be seen that the fuel cell has the highest specific energy, while the specific power is the lowest compared the other energy sources. Each energy source has its own advantages and disadvantages, so many researchers have also sought to combine those energy sources with their advantages to create hybrid power sources. For example, a hybrid power source could be a combination of a battery and a fuel cell that can take advantage of the battery's high-power density, high efficiency, fast response, and advantages of the fuel's high energy density. In this case, the battery is used as the power source for the request of peak power, such as takeoff and climbing. Additionally, the fuel cell could be used in the cruise and descent periods.

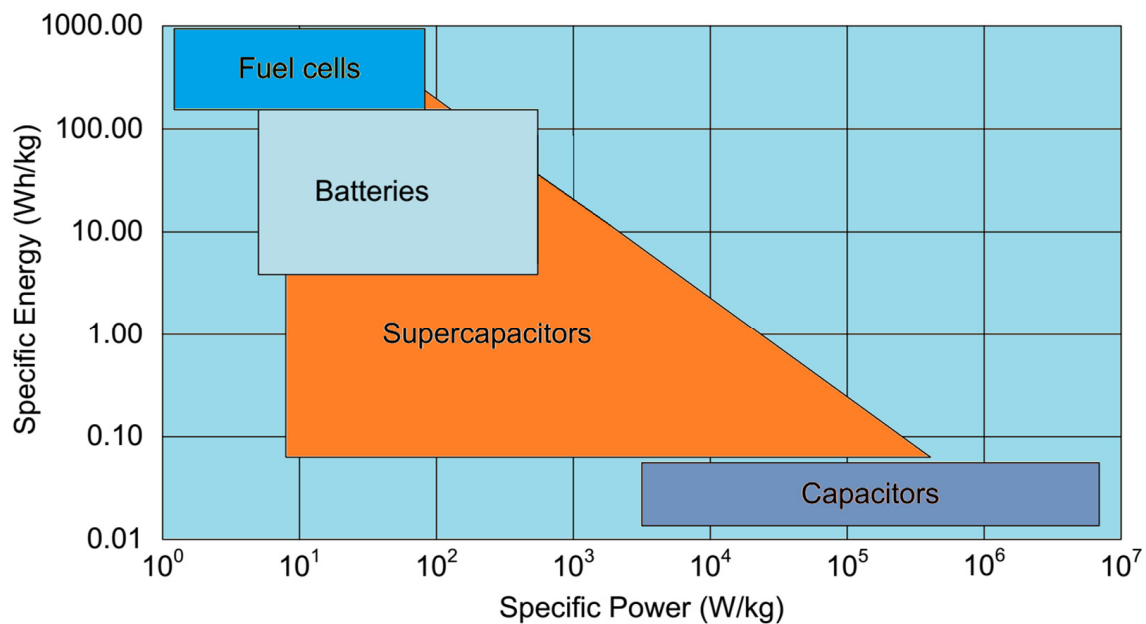


Figure 12. Comparison between energy sources [38].

Another approach that is of interest to researchers is to use external energy sources, such as solar energy and wind power, to increase the endurance of the UAV without the need to return to the ground for recharging. That helps UAVs to be more efficient in performing their tasks. Solar-powered UAVs (especially fixed-wing UAVs) convert energy from sunlight into electricity by using photovoltaic panels installed on the wings. Some UAVs that use solar energy as a source of energy could be mentioned, such as NASA's Pathfinder [39], Helios [40], and Airbus Zephyr developed by Qinetiq Inc. [41]. One of the disadvantages of solar-powered UAVs is that they are only efficient during the day. At night or when it is cloudy, the amount of electricity obtained from photovoltaic panels is absent or negligible. Wind energy is one of the clean and available energy sources in nature. There have been many research works on applying wind power in many different areas of life [42]. However, the conversion of wind energy into electricity to provide operational power for UAVs is still limited. In this paper, we focus on analyzing the possibility of recharging energy using wind energy in UAVs.

#### 2.4. Charging Techniques for Battery Used in UAVs

By using chemicals to absorb and release energy on demand, batteries are the most popular energy storage devices in UAVs due to their many advantages. Among the traditional charging methods, battery swapping is the most widely used on UAVs. However, nowadays, wireless charging is increasingly attracting the attention of researchers. Approaches to wireless charging can be divided into two groups: non-EMF-based charging and EMF-based charging.

**The non-EMF-based technique** mainly includes gust soaring, PV array, and laser beaming (shown in Figure 13). *Gust soaring* is one of the non-EMF-based techniques to help increase the flight time of UAVs. By adjusting the trajectory of the UAV to catch the rising air, it can convert wind energy into the energy needed for the UAV's operation (shown in Figure 13a). In [43] the authors proposed a numerical analysis of dynamic soaring. However, this technique still has some drawbacks that this method is only effective for fixed-wing UAVs and is highly wind dependent.

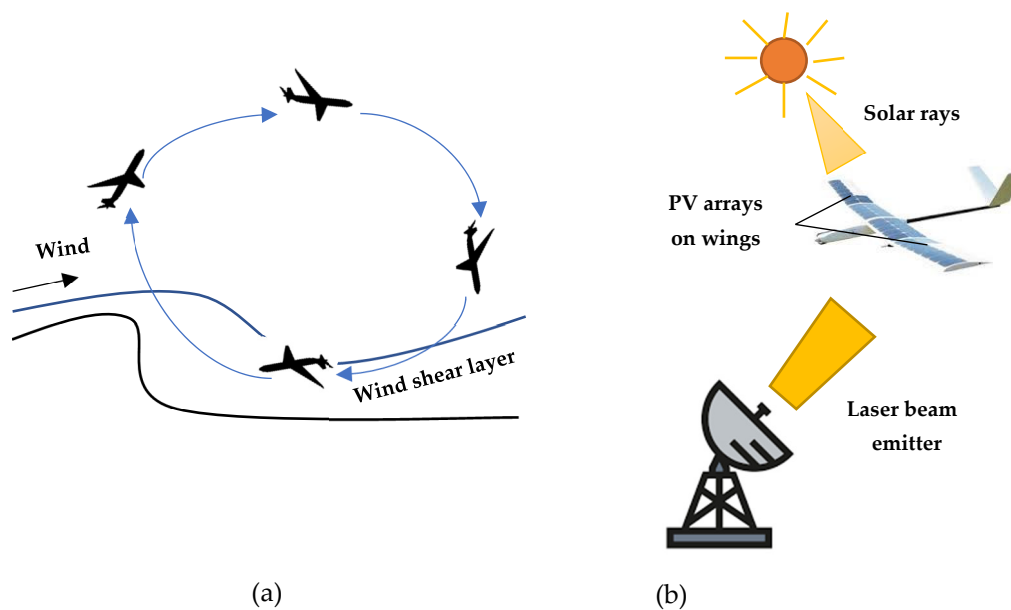


**Figure 13.** Non-EMF-based techniques: (a) gust soaring; (b) PV arrays and laser beaming.

*PV arrays* is a technique that uses photovoltaic panels to convert solar radiation into electricity. Researchers have focused on studying the factors affecting the efficiency of electricity conversion from solar energy. Many studies have shown that factors such as the arrangement of photovoltaic cells, flight time, battery type, and payload are the most important parameters, while the efficiency of the photovoltaic cell and the electrical components do not play a crucial role [44]. *Laser beaming* is a technique commonly used by the military to prolong the flight time of UAVs for reconnaissance or intelligence purposes [45]. In [46–48], laser, which, in the form of a concentrated and streamlined beam of light at a certain frequency and of a particular wavelength, is directed to photovoltaic cells, was installed on a UAV. This PV cell will convert the laser beam into useful energy to recharge the battery of the drone. Besides those non-EMF-based techniques, *battery dumping* is also considered another technique to prolong the UAV's mission duration. This strategy helps to increase the mission duration of the aircraft marginally. In [49], the authors proposed a concept of decreasing the UAV weight by dumping empty battery packs and, consequently, slightly increasing the UAV's flight time. They divided the battery pack into sections, connected them, and detached sections once they were fully discharged. In [50], the authors gave other solutions to implementing automated battery changing stations. The empty battery is removed from the UAV with the help of automated manipulators at a specifically designed platform, while a new fully charged battery is replaced.

**EMF-based techniques** are also considered one of the options, which can be used to increase the UAV's mission duration. In [51], the authors researched the potential of using the power line's electromagnetic field to charge a UAV and proposed a method to estimate the amount of energy available for the UAV to use around the transmission line by using a magnetic field. In [52], capacitive, inductive, and magnetic resonant charging techniques were presented. In this technique, the problems of the UAV's battery recharging and high efficiency of the power transfer during the movement are still challenging tasks.

Current charging techniques are commonly used on fixed-wing UAVs, while rotary wings are limited. In Table 1, it is mentioned that rotary wing has higher power consumption than other types of UAV. Among the types of rotary wing, the quadrotor is the type of UAV that has the most applications in both civil and military applications, thanks to its many advantages. However, the problem of supplying power to ensure the quadrotor can operate for a longer time is still a big challenge. In the next section, we will discuss the dynamic model, the control methods of the quadrotor, and the method of taking advantage of wind energy to convert it to electrical energy for a quadrotor.

### 2.5. Working Principle and Dynamic Model of a Quadrotor

Multicopters are widely used in the world because of their versatile flight flexibility. The multicopter can perform complex movements by changing the speeds of the motors. Among them, the quadrotor is the most popular drone that has many advantages, such as cheap cost, compact size, ease of control. The quadrotor moves mainly because of the thrusts from the four motors fixed symmetrically to the platform. To be able to control the quadrotor, every two opposite motors (1, 3 and 2, 4) must rotate in the same direction, and the other two are on the contrary. A model of a quadrotor is illustrated in Figure 14.

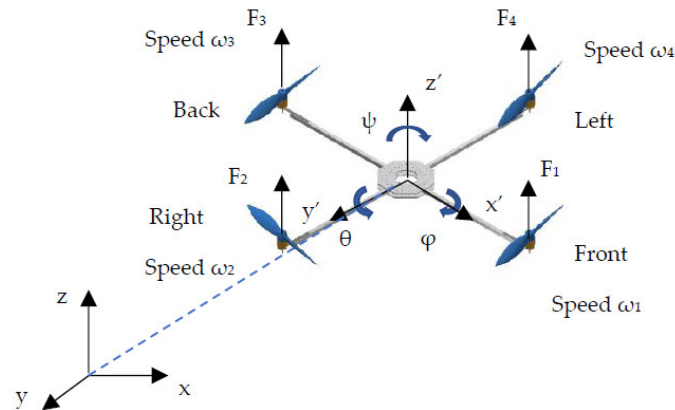


Figure 14. Quadrotor configuration.

The motors are supplied with different amperages, which will change the force and torque balances on the quadrotor.

#### 2.5.1. Quadrotor’s Dynamic Modeling

The Euler-Lagrange formalism is used to model the dynamic rotation of a quadrotor. The airframe orientation can be given by a rotation,  $R_{B-E}$ , from a body-fixed frame to an earth-fixed frame, where  $R_{B-E}$  is the rotation matrix.

Using the Lagrange method, the motion equation can be written in a general form:

$$G_i = \frac{d}{dt} \left( \frac{\delta L}{\delta \dot{q}_i} \right) - \frac{\delta L}{\delta q_i} \tag{4}$$

where  $q_i$  are generalized coordinates, and  $G_i$  are generalized forces.

$q_i = (x, y, z, \varphi, \theta, \psi) \in R^6$ , where  $(x, y, z) \in R^3$  are absolute positions of the quadrotor mass in a fixed-body frame.  $(\varphi, \theta, \psi) \in R^3$  are Euler angles, where  $\varphi, \theta, \psi$  are roll, pitch, and yaw angles respectively.

To calculate parameters of the quadrotor between two frames, the rotation matrix can be obtained by the following formula:

$$R = \begin{bmatrix} C_\psi C_\theta & C_\psi S_\theta S_\phi - C_\phi S_\psi & C_\psi S_\theta C_\phi + S_\phi S_\psi \\ S_\psi C_\theta & S_\psi S_\theta S_\phi + C_\phi C_\psi & S_\psi S_\theta C_\phi - S_\phi C_\psi \\ -S_\theta & C_\theta S_\phi & C_\theta C_\phi \end{bmatrix} \tag{5}$$

where  $C^* = \cos(*)$  and  $S^* = \sin(*)$ .

The kinematic energy can be calculated as:

$$T = \frac{1}{2} I_{xx} (\dot{\varphi} - \dot{\psi} \sin \theta)^2 + \frac{1}{2} I_{yy} (\dot{\theta} \cos \varphi + \dot{\psi} \sin \varphi \cos \theta)^2 + \frac{1}{2} I_{zz} (\dot{\theta} \sin \varphi - \dot{\psi} \cos \varphi \cos \theta)^2 \tag{6}$$

where  $I_{xx}, I_{yy}, I_{zz}$  are moments of inertia on the axes  $x, y$ , and  $z$ , respectively.

The potential energy can be calculated as:

$$V = g \int x dm(x)(-g \sin \theta) + \int y dm(y) g \sin \varphi \cos \theta + \int z dm(z) g \cos \varphi \cos \theta \tag{7}$$

Using Lagrangian formula  $L=T-V$ , the three equations of motion can be received:

$$\begin{cases} I_{xx} \ddot{\phi} = \dot{\theta} \dot{\psi} (I_{yy} - I_{zz}) \\ I_{yy} \ddot{\theta} = \dot{\phi} \dot{\psi} (I_{zz} - I_{xx}) \\ I_{zz} \ddot{\psi} = \dot{\theta} \dot{\phi} (I_{xx} - I_{yy}) \end{cases} \tag{8}$$

Each BLDC motor generates a thrust moment, which is defined by  $T_i = b\omega_i^2$ , where  $b$  is a thrust factor of the propeller and  $b > 0$ .  $\omega_i$  is an angular velocity of the motor  $i$ .

The main thrust acting on the quadrotor is the summation of thrust moments of four motors that can be calculated by the following formula:

$$T = T_1 + T_2 + T_3 + T_4 \tag{9}$$

The generalized moments can be obtained by the following formula:

$$\begin{cases} \tau_x = bl(\omega_4^2 - \omega_2^2) \\ \tau_y = bl(\omega_3^2 - \omega_1^2) \\ \tau_z = d(\omega_1^2 + \omega_3^2 - \omega_2^2 - \omega_4^2) \end{cases} \tag{10}$$

where  $l$  is the distance from the motor to the quadrotor center mass, an  $d$  is the drag factor.

The control from motors can be obtained as follows:

$$\begin{bmatrix} T \\ \tau_x \\ \tau_y \\ \tau_z \end{bmatrix} = \begin{bmatrix} b & b & b & b \\ 0 & -bl & 0 & bl \\ -bl & 0 & bl & 0 \\ d & -d & d & -d \end{bmatrix} \begin{bmatrix} \omega_1^2 \\ \omega_2^2 \\ \omega_3^2 \\ \omega_4^2 \end{bmatrix} \tag{11}$$

The dynamic model of the quadrotor is introduced as follows:

$$\begin{bmatrix} \ddot{x} \\ \ddot{y} \\ \ddot{z} \end{bmatrix} = \begin{bmatrix} (C_\psi S_\theta C_\phi + S_\phi S_\psi) K_1 \\ (S_\psi S_\theta C_\phi - S_\phi C_\psi) K_1 \\ -g + C_\theta C_\phi \end{bmatrix} \tag{12}$$

$$\begin{bmatrix} \ddot{\phi} \\ \ddot{\theta} \\ \ddot{\psi} \end{bmatrix} = \begin{bmatrix} \dot{\theta} \dot{\psi} \left( \frac{I_{yy} - I_{zz}}{I_x} \right) - \frac{J_r}{I_{xx}} \dot{\theta} \Omega \\ \dot{\phi} \dot{\psi} \left( \frac{I_{zz} - I_{xx}}{I_{yy}} \right) + \frac{J_r}{I_{yy}} \dot{\phi} \Omega \\ \dot{\theta} \dot{\phi} \left( \frac{I_{xx} - I_{yy}}{I_{zz}} \right) \end{bmatrix} + \begin{bmatrix} \frac{1}{I_{xx}} & 0 & 0 \\ 0 & \frac{1}{I_{yy}} & 0 \\ 0 & 0 & \frac{1}{I_{zz}} \end{bmatrix} \begin{bmatrix} K_2 \\ K_3 \\ K_4 \end{bmatrix} \tag{13}$$

The control inputs  $K_1, K_2, K_3$ , and  $K_4$  can be obtained:

$$K_1 = b(\omega_1^2 + \omega_2^2 + \omega_3^2 + \omega_4^2) \tag{14}$$

$$T = \begin{bmatrix} K_2 \\ K_3 \\ K_4 \end{bmatrix} = \begin{bmatrix} bl(\omega_4^2 - \omega_2^2) \\ bl(\omega_3^2 - \omega_1^2) \\ d(\omega_1^2 + \omega_3^2 - \omega_2^2 - \omega_4^2) \end{bmatrix} \in R^3 \tag{15}$$

where,  $K_1$  is an essential parameter to control the quadrotor reaching the desired attitude;  $K_2, K_3, K_4$  control the roll, pitch, and yaw displacement, respectively;  $J_r$  is the moment of inertia of the rotor; and  $\Omega$  is the overall sum of rotors' speed.

To control the quadrotor, we use the semiphysical DSPACE system. With the DSPACE system, it is possible to receive signals from sensors and output PWM signals to control the motor speed. However, in order to control the quadrotor, it is necessary to first mention

about its control methods. In the next section, we will briefly discuss the control methods commonly used on the rotary wing in general and the quadrotor in particular.

### 2.5.2. Control Methods for the Quadrotor

Since the appearance of UAVs, many control methods for UAVs have been researched and developed over the years to make the control response faster, less erroneous, and more accurate. The control methods can be divided into three main groups: Linear robust control, nonlinear control, and intelligent control.

The linear robust control method was found early in the quadrotor development and was sufficient for stable flight. Some linear robust control can be mentioned, such as the proportional–integral–derivative controller (PID), which is known as one of the most popular controllers due to its ease of application and simplicity (see Figure 15). In control theory, one of the classical approaches is PID controller. The PID controller has many advantages compared with other controllers in some aspects, such as great ease of implementation, ease of changing parameters (gains), and reliable algorithm yield.

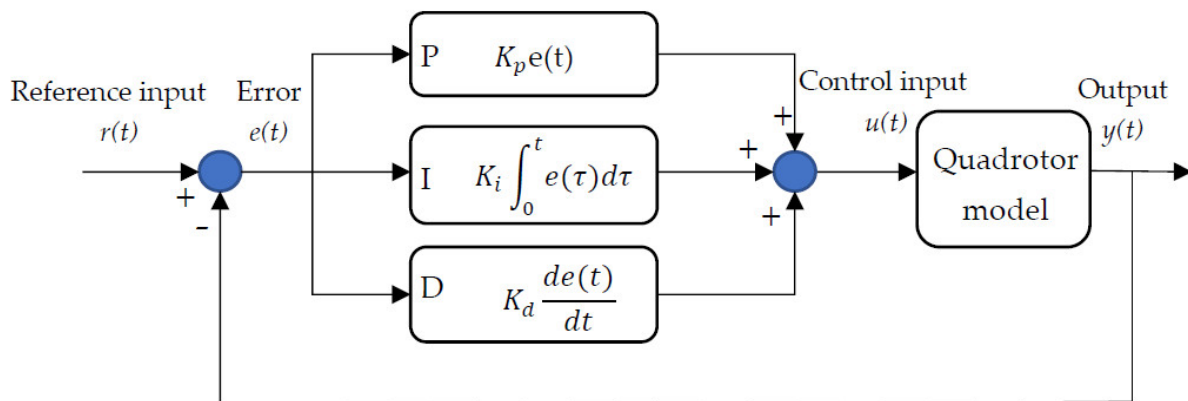


Figure 15. Block diagram of a PID controller.

The overall control function is introduced:

$$u(t) = K_p e(t) + K_i \int_0^t e(\tau) d\tau + K_d \frac{de(t)}{dt} \quad (16)$$

**Linear quadratic controller.** In the quadrotor control, the commonly used LQ controllers are the linear quadratic regulator (LQR) and linear quadratic Gaussian (LQG) controllers. To optimize the system, a cost function and a minimum cost by a weighting factor are used. *The  $H_\infty$  controller* is commonly used in the quadrotor system with external disturbances and uncertainties. It can achieve stabilization with a guaranteed performance by synthesizing controllers; hence, many researchers try to apply the  $H_\infty$  controller to a quadrotor control.

Since a quadrotor is a system with many inputs and 6 degrees of freedom, *nonlinear controllers* are often used to have better performance. Nonlinear controllers can be mentioned as backstepping control techniques, feedback linearization, and sliding mode control. The *feedback linearization controller* is used to transform the nonlinear system into an equivalent linear system by changing the variables and suitable control input. A nonsingular matrix can be obtained by using a similarity transformation. Then the system can be applied a standard linear control theory. After that, the solution can be used in the nonlinear system. The *backstepping controller* is used for a special class of nonlinear dynamics systems. Using other methods can stabilize the subsystems that are from an irreducible subsystem. The design process can begin from a known-stable system and “back out” new controllers that progressively stabilize each of the subsystems. When the final external control is reached, the process will complete. The *sliding mode controller* (SMC) modifies the system using a discontinuous control signal to force the system moving within the system’s normal

behavior. Because of model uncertainties and external disturbances, the SMC technique changes the system to the sliding surface.

Compared with other control strategies, *intelligent control* covers a wide range of uncertainties. Intelligent controllers can be mentioned, such as fuzzy logic controller, model predictive, and neural network controller. *The fuzzy logic controller* has advantages over another controller as human experience can be used to design controller. A fuzzy controller consists of an input stage, an output stage, and a processing stage. Triangle is the most common shape of the membership function. In [53], the authors used fuzzy logic control with PID and LQR control to control a quadrotor with a Qball-X4 platform. *The neural network* consists of neurons, which interact with each other in different layers. The neural network system has units called processing elements. The neural network is used for the design of a nonlinear dynamic system with uncertain nonlinear terms and system errors. *The model predictive controller* (MPC) is used to predict the future behavior of the system to optimize a cost function by generating the future control input. The MPC is considered an advanced process control method for maintaining the output at the operational conditions and set points.

A quadratic cost function for optimization is given by:

$$J = \sum_{i=1}^N w_{x_i} (r_i - x_i)^2 + \sum_{i=1}^N w_{u_i} \Delta u_i^2 \quad (17)$$

In [54], a neural network and an MPC were used to control the quadrotor to chase an escaping target in cluttered environments. The authors proposed a GTO-MPC-based practical framework to generate chasing trajectories for the quadrotor. In [55], the authors used nonlinear MPC for a fault-tolerant controller to stabilize and control a quadrotor with a single broken rotor.

From the above control methods, the authors built a set of experiments to control the quadrotor to perform different flight scenarios to evaluate the energy consumption of the UAV.

### 3. Development of Accumulation to Improve Energy Consumption in the Quadrotor

#### 3.1. Energy Accumulation by Wind Energy Conversion

##### 3.1.1. Concept of Energy Conversion from Wind Energy to Electrical Energy in the Quadrotor

Wind energy is one of the clean and available energies in nature. Using regenerative braking mode, many researchers have tried to convert wind energy into electrical energy to power a UAV. In principle, under the action of air flowing through the blade, the propeller rotates and turns the motor into a generator (see Figure 16). There are two options that can generate power on a quadrotor: using a nonvariable pitch propeller and a variable pitch propeller.

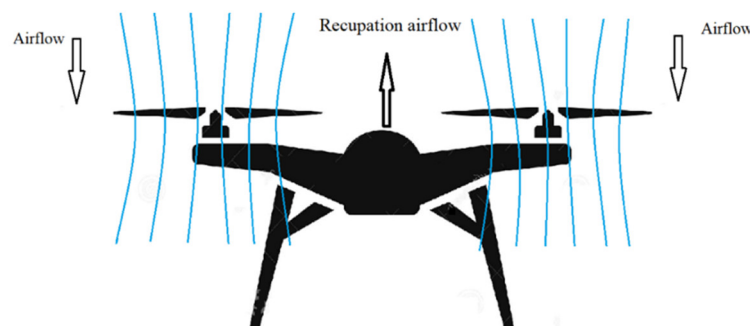


Figure 16. Air direction on charging mode [56].

In the case of a nonvariable pitch propeller, the direction of the rotation of the propeller in motorized mode will be opposite to that of the propeller in regenerative braking mode. As soon as the motors of the UAV are disconnected, the rotation of the propeller will slow down and stop. When the UAV decreases in altitude, the wind will affect the propeller, causing it to rotate in the opposite direction and cause the motor to become a generator and charge it back. However, the efficiency of this energy charging is not high when the wind energy has lost a large amount to stop the rotation of the propeller.

In the case of a variable pitch propeller (VPP), the VPP changes the angle of attack to keep the same direction of rotation. This regime of autorotation can generate much more electrical energy than static propellers, and it is far easier to control the flight itself (see Figure 17).



**Figure 17.** UAVs with variable pitch propellers [57].

The technique of using wind energy to generate electrical energy through regenerative braking mode is not all common in a multirotor. The above-mentioned pitch propeller possibilities of power generation use techniques that are, however, not at all common. Most of the multirotor drones used nowadays do not have variable pitch propellers, and using the reverse flow of the air is impossible without the need for reprogramming the flight controller. However, for the classic airplane, both methods are applicable in real situations. Therefore, the goal is to evaluate the effectiveness of energy generation in regenerative braking mode.

### 3.1.2. Winding Energy Conversion of the BLDC Motor

The structure of a BLDC motor drive system is shown in Figure 18. In this topology, the voltage of the battery is proposed to be  $V_{\text{Batt}} < V_{\text{sc}}$  (voltage of a supercapacitor). Under normal conditions, the diodes  $D_1$  and  $D_2$  are reverse-biased. In this case, the battery and supercapacitor power the UAV's electric propulsion system by supplying the BLDC motors with suitable voltages. The controller uses rotor position signals recognized by Hall sensors to control the switches  $K_{1-6}$  to produce continuous torque. The conversion of wind energy to electrical energy occurs with the regenerative braking event. The  $D_1$  is forward-biased, and the supercapacitor could harvest the braking energy through the inverter. When the voltage of the supercapacitor ( $V_{\text{sc}}$ ) is greater than the upper voltage limit of the supercapacitor ( $V_{\text{scmax}}$ ), the regenerative energy stops flowing into the capacitor, and then it goes to the battery through  $D_2$ , which is in a state of forward bias. In regenerative braking mode, the MOSFETs on the high side of the H-bridge are turned off, and those on the low side are controlled by an appropriate PWM. By using a suitable switching scheme, the bidirectional switches and the utilization of the inductances in the BLDC motor and the inverter can be used as a boost circuit to change  $D_1$  and  $D_2$  states and, thus, the BLDC motor modes.

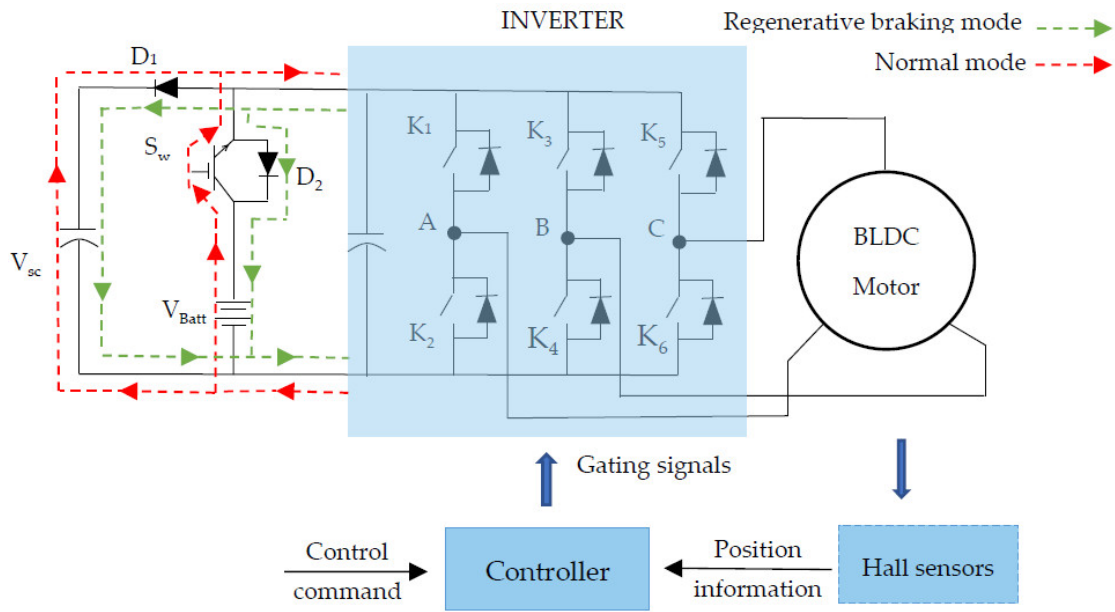


Figure 18. BLDC motor drive system with normal mode and regenerative braking mode.

3.2. Experiment for Evaluating Energy Consumption

3.2.1. System Design and Manufacture for Control Testing and Data Acquisition

The system was first designed in Inventor (shown in Figure 19). Using tools in Inventor can find out relatively accurate system parameters, such as moments of inertia ( $J_{xx}$ ,  $J_{yy}$ ,  $J_{zz}$ ) around the axes x, y, and z.

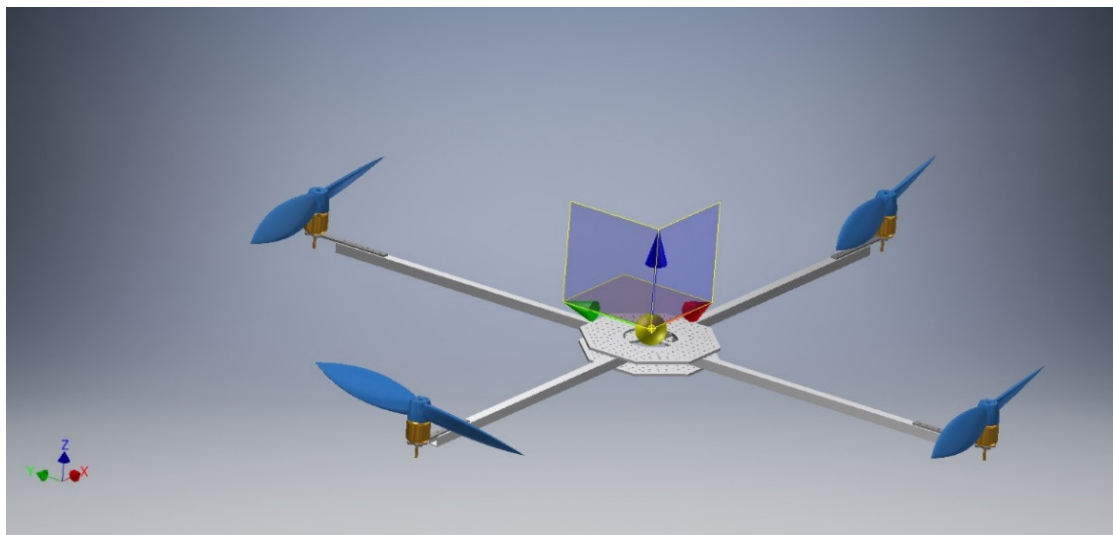


Figure 19. Quadrotor design in Inventor.

Then, the system is built with a rigid frame that can slide vertically with very little friction. Four motors are attached to four corners of the cross-shaped frame. The distance from each motor to the center is 65 cm. The bar connecting the motor to the center is made of aluminum with a thickness of 1 mm. The frame is punched with many small holes to reduce the weight of the system and provide better wiring. The basic system parameters are shown in Table 2.

**Table 2.** System parameters.

Parameters	Value	Unit
$I_{xx}$	0.23	kg.m <sup>2</sup>
$I_{yy}$	0.23	kg.m <sup>2</sup>
$I_{zz}$	0.449	kg.m <sup>2</sup>
$I_r$	0.0021	kg.m <sup>2</sup>
Mass	2.1	kg
Length	0.65	m
Thrust coefficient	$3.68 \cdot 10^{-5}$	N.s <sup>2</sup>
Drag coefficient	$1.61 \cdot 10^{-6}$	N.m.s <sup>2</sup>

The state parameters of the quadrotor measured by using the sensors MPU 6050 and HY-RS05 are sent to the computer via Arduino Uno and the dSPACE system. dSPACE is a semiphysical simulation system in which the quadrotor's controller will be simulated in a Simulink environment. By using the DS1104SL\_DSP\_PWM block, it is possible to directly output the PWM signal through the ports ST2PWM, SPWM7, SPWM8, and SPWM9 to control the motors' speed. The dSPACE ControlDesk program uses the sdf file, which is generated from a MATLAB file to monitor and edit system parameters in real time (shown in Figure 20).

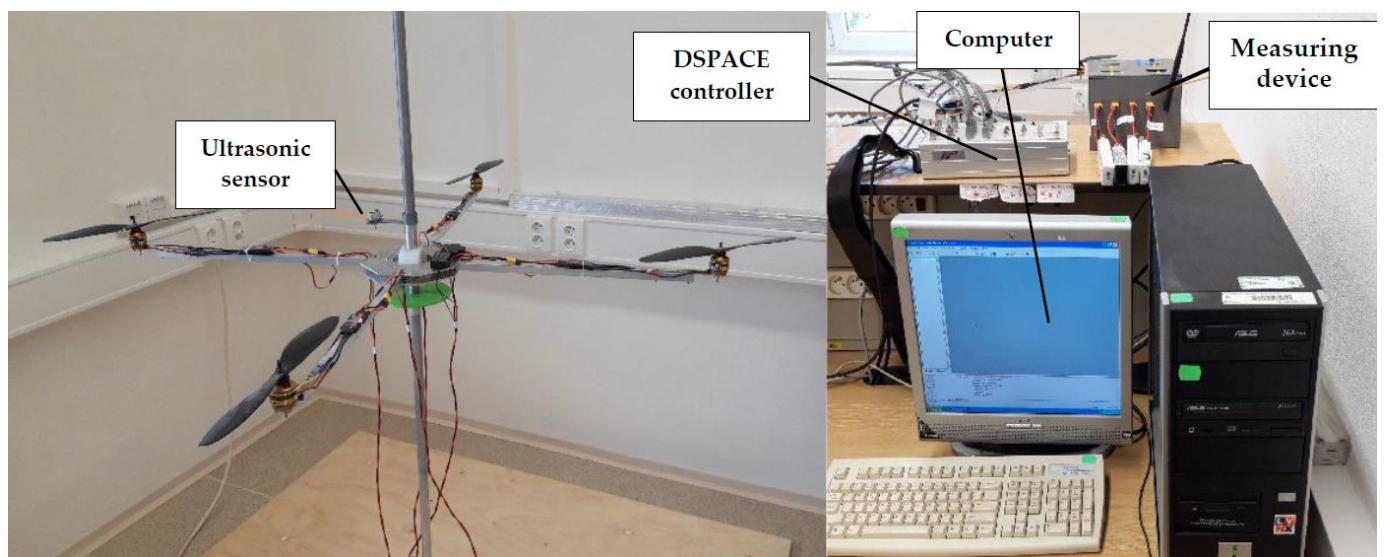
**Figure 20.** Test bench of regenerative braking UAVs to design control.

Figure 21 shows dSPACE's interface. It mainly has three parts. The system parameter sections include altitude, vertical speed, and yaw, which are measured by MPU 6050 and HY-RS05 and sent to dSPACE using Arduino Uno via NRF24L01. The second section shows the values of current motors and battery voltages that are measured by the measuring device. The data acquisition section is for collecting data of various parameters of the system and can help to save them into a log file, which can be used later in MATLAB.

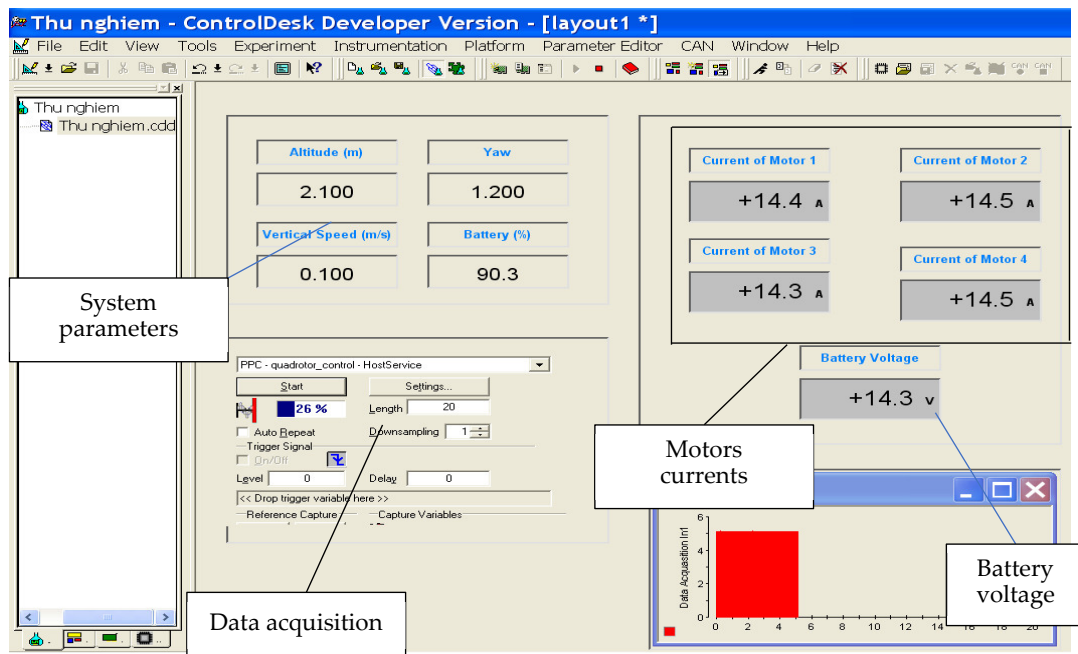


Figure 21. dSPACE’s interface.

### 3.2.2. The Measuring Device

The measuring device is designed to measure and monitor the voltages and currents of four motors at the same time. The measurement data are transmitted directly to the computer via a Wi-Fi network to serve the purposes of calculation and system simulation. The operating principle of the measuring device is shown in Figure 22.

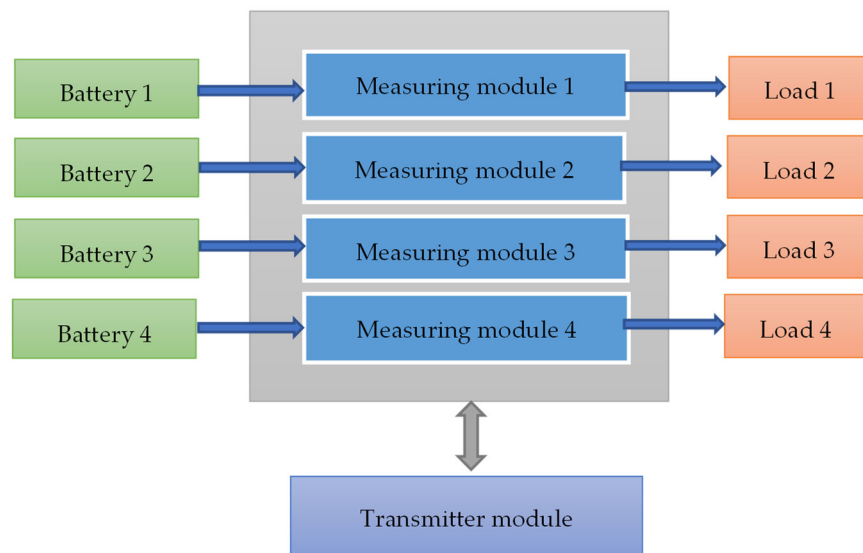
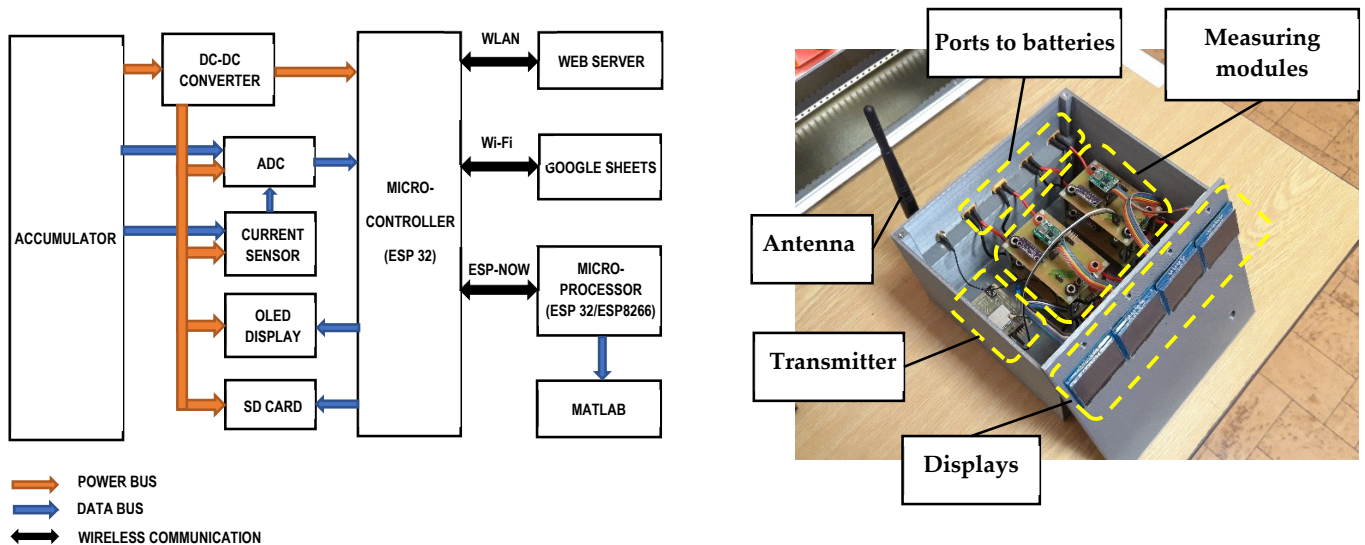


Figure 22. The operating principle of the measuring device.

The measuring device consists of four measuring modules. Each measuring module has a structure shown in Figure 23. The measuring device uses a microprocessor, ESP32, in collecting and processing data from the current and voltage at the same time and sending them to the computer in real time. The dual-core ESP32 is used to make the system work fluently. Core 0 is in charge of measuring the accumulator’s current and voltage, calculating the state of charge (SoC), recording data to the SD card, and displaying to the OLED display. Then, Core 0 will calculate the data, which later will be sent to the computer via a wireless

channel by Core 1. If the transmission is unsuccessful, it must be repeated by Core 1 without effect on the measurement process of Core 0.



Block diagram of a measuring module

Measuring device

Figure 23. The measuring device [58].

In addition, on the measuring device, there are four screens that simultaneously display parameters, such as the amperage, voltage, temperature, and power consumption of each motor.

The measuring modules are calibrated with the help of the multimeter Agilent 34410A and 34330A 30 A Current Shunt. The device has a relative error of 0.3% in the case of voltage measurement and 3% in the case of current measurement.

### 3.3. Experiment to Generate the Maximum Efficiency of Wind Energy to Electric Energy Conversion

The second experiment was conducted to determine the efficiency parameters of the system in the aerodynamics laboratory of the Department of Aviation Technology at the University of Defence, Brno. To simulate different wind speeds, an electric motor with a power of 18 kW and a fan diameter of 50 cm was installed in the wind tunnel. The operating range of the subsonic wind tunnel was from 2 to 42 m/s. Test conditions and parameters of the components used in the experiment are shown in Table 3.

Table 3. Test conditions and parameters of the components used in the experiment.

	Parameters	Value	Unit
Experimental condition parameters	Atmospheric pressure	745.2	mmHg
	Temperature	24.8	°C
	Air density	1.1595	Kg/m <sup>3</sup>
Motor KV380	Rated voltage	4–6	S
	Internal Resistance	194	mΩ
	Weight	68	g
Carbon fiber Propeller	Diameter	16	Inches
	Pitch	5.5	Inches
Power slide-type potentiometers	Max resistance	105	Ω

In generating mode, the coefficient of ratio speed can be calculated by the following formula:

$$\lambda_0 = \frac{\pi \cdot D \cdot n_s}{V_0} \quad (18)$$

Drag can be calculated by the following formula:

$$T = \frac{1}{8} c_f \rho \pi D^2 V_0^2 \quad (19)$$

where  $c_f$  is the drag coefficient.

Torque can be calculated by the formula:

$$M = \frac{1}{16} c_m \rho \pi D^3 V_0^2 \quad (20)$$

where  $c_m$  is the torque coefficient.

The power supply by the wind onto the system can be calculated by the following:

$$P_w = \frac{1}{8} c_p \rho \pi D^2 V_0^3. \quad (21)$$

where  $c_p$  is the power coefficient

The total power can be calculated by the following:

$$P_{total} = P_1 + P_2 + P_3 \quad (22)$$

where  $P_{total}$  is the instantaneous total power from three channels of the motor.

$P_1$ ,  $P_2$ , and  $P_3$  are instantaneous powers of channels 1, 2, and 3, respectively.

The efficiency of wind energy to electric energy conversion can be calculated by the following.

$$\eta_0 = \frac{P_{total}}{P_w} \quad (23)$$

Figure 24 shows the diagram of the experimental setup. The electric motor with a  $16 \times 5.5$  propeller is placed perpendicular to the airflow in the wind tunnel. They are connected in series with three potentiometers.

The experiment was conducted with wind speeds of 12 and 15 m/s. The test modes were symmetrical and asymmetrical loads (potentiometers). The data were measured with instruments of the company NI and the program LabVIEW. Computer 1 was responsible for controlling the aerodynamic parameters, temperature, and so on, of the wind tunnel. Computer 2 connected to computer 1 was responsible for processing measured parameters from measurement block 2 to calculate and display values, such as power, amperage, and the voltage of each phase.

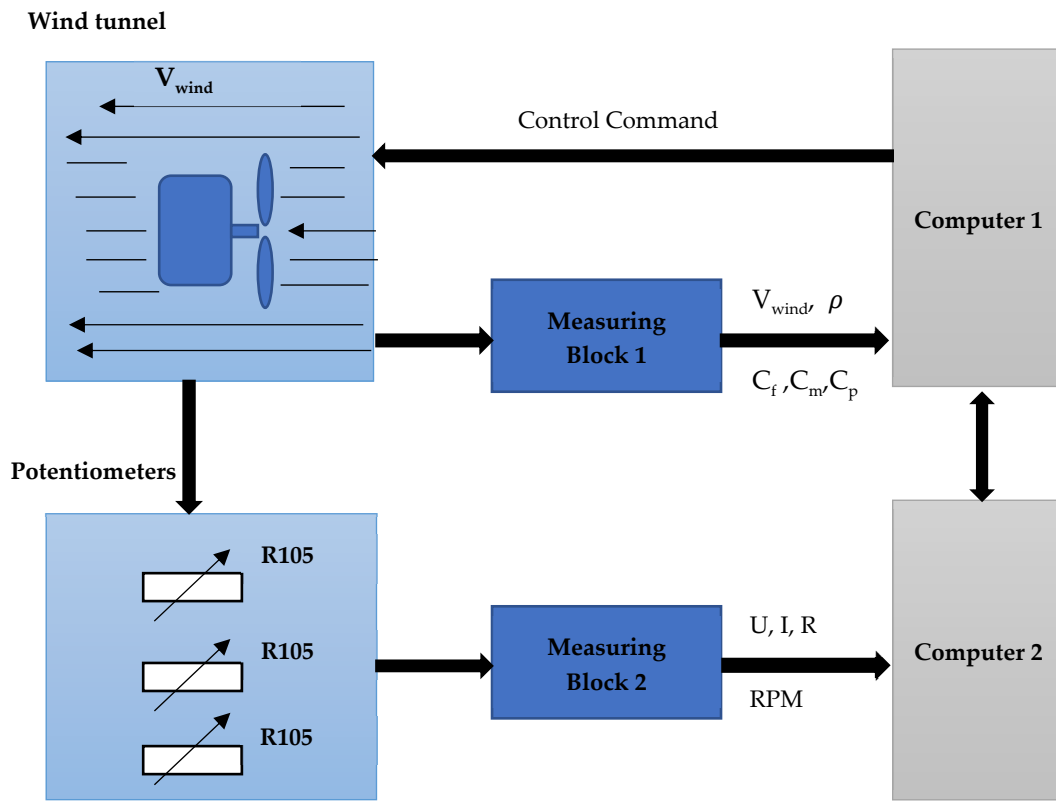


Figure 24. Diagram of the experimental setup.

#### 4. Experimental Results and Discussion

##### 4.1. First Experiment

In this experiment, the system conducted three consecutive tests to evaluate the energy consumption parameters of the system at different heights of 1, 2, and 2.5 m. Figure 25 shows the measured voltage and current of the system. On the first flight, the flight time was 26 s. The amperage before takeoff was 0.6 A and quickly peaked at 80 A. The voltage of the battery was reduced to 14 V during the flight of the system. The energy consumed for the first flight was about 6 Wh.

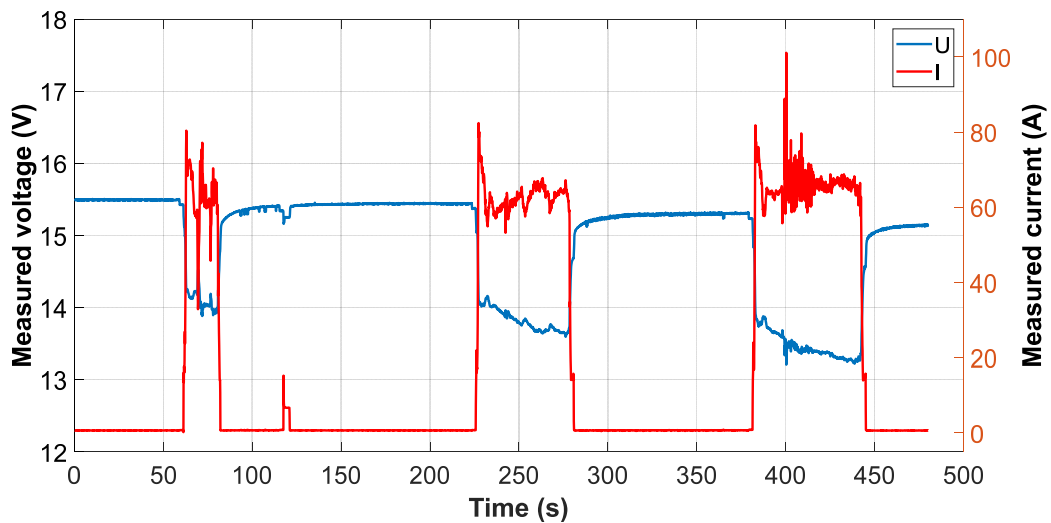


Figure 25. Measured voltage and current of the system.

The second flight had a flight that lasted up to 55 s. The battery voltage at the start of the second flight was 15.37 V in comparison with 15.49 V of the first flight. During the flight, the battery voltage dropped to as low as 13.65 V, and at the end of the flight, it recovered to 15.2 V. The energy consumed for this flight was approximately 13 Wh. In the case of the third flight, the flight time of the system was 54 s. Around the 400th second, the amperage suddenly increased to nearly 100 A because, during the flight, the system performed the flight to a height of more than 0.2 m and then returned to a height of 2.5 m. The amount of energy the system consumed was 15.5 Wh in this third flight. The voltage of the battery dropped to the lowest value of 13.3 V and returned to the value of 15.1 V (see Figure 26).

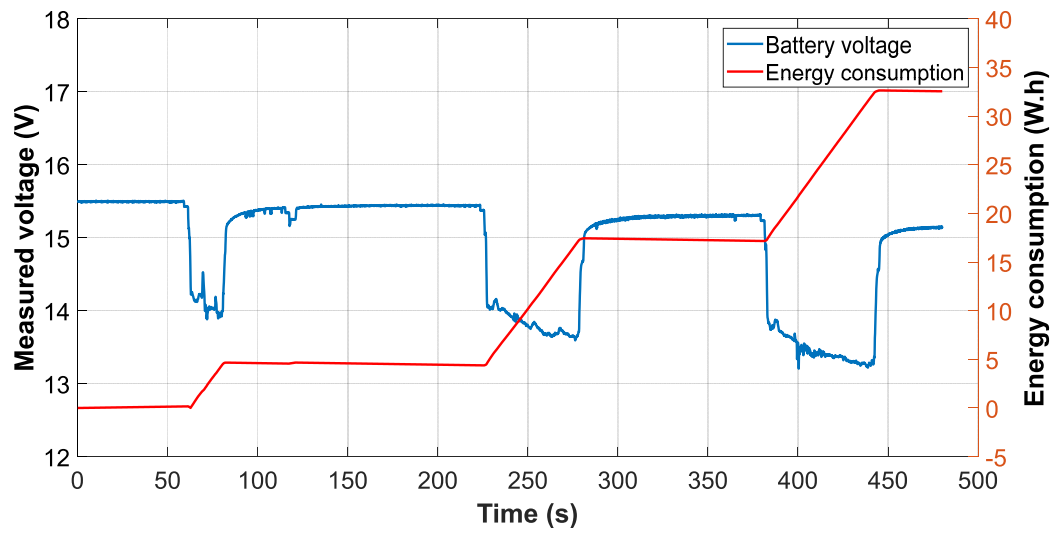


Figure 26. Energy consumption of the system.

#### 4.2. Second Experiment

In Figure 27,  $P_{t1}$  and  $P_{t2}$  are total powers in the case of symmetrical load and asymmetrical load, respectively.  $C_{p1}$  and  $C_{p2}$  are power coefficients in the case of symmetrical load and asymmetrical load.

In Figure 27a, the value of the total powers obtained from the experiment with a wind speed of 12 m/s increased and reached the maximum values of 4.4 and 4.1 W as the coefficients of ratio speed had values of 3.3 and 3.31, respectively. In Figure 27b, in the case of a wind speed of 15 m/s, the maximum values of the total powers that can be obtained were 9 and 10.1 W. By using Equations (18)–(23), it was possible to calculate the efficiency of wind energy to electric energy conversion. Figure 27 shows a comparison of the coefficient of efficiency  $\eta_o$  in the cases of symmetrical and asymmetrical loads of a three-phase generator.

It can be seen from Figure 28 that the coefficient of efficiency in the case of symmetrical load became a better value in comparison with the case of asymmetrical load. With a wind speed of 12 m/s, the coefficient of efficiency reached the highest values of 37.2% and 42.8% when the coefficients of ratio of speed ( $\lambda_0$ ) were 1.55 and 3.1, respectively. In Figure 28, the maximum values of the coefficients of efficiency were 49.1% and 47.3 as  $\lambda_0 = 3.44$  and  $\lambda_0 = 2.91$ , respectively, in the case of a wind speed of 15 m/s.

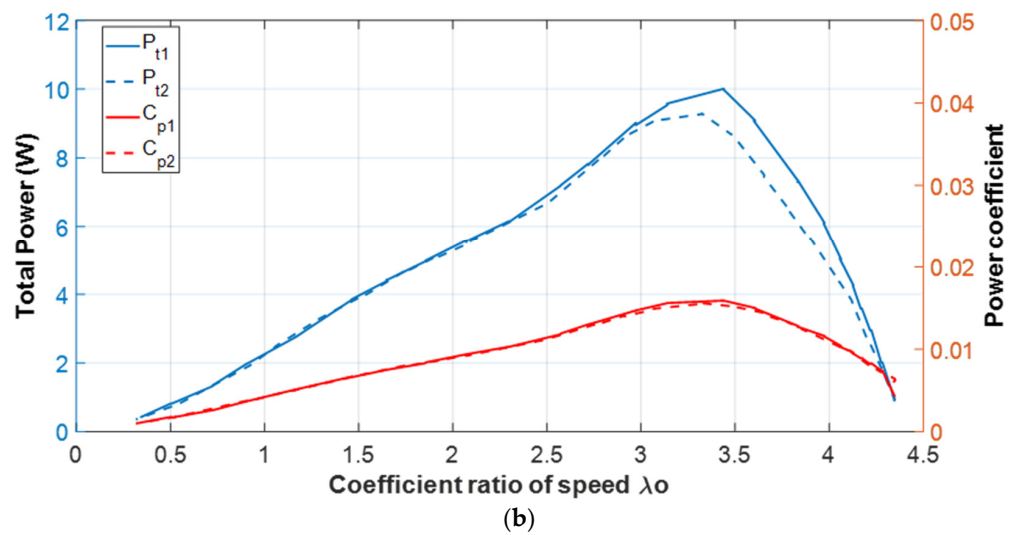
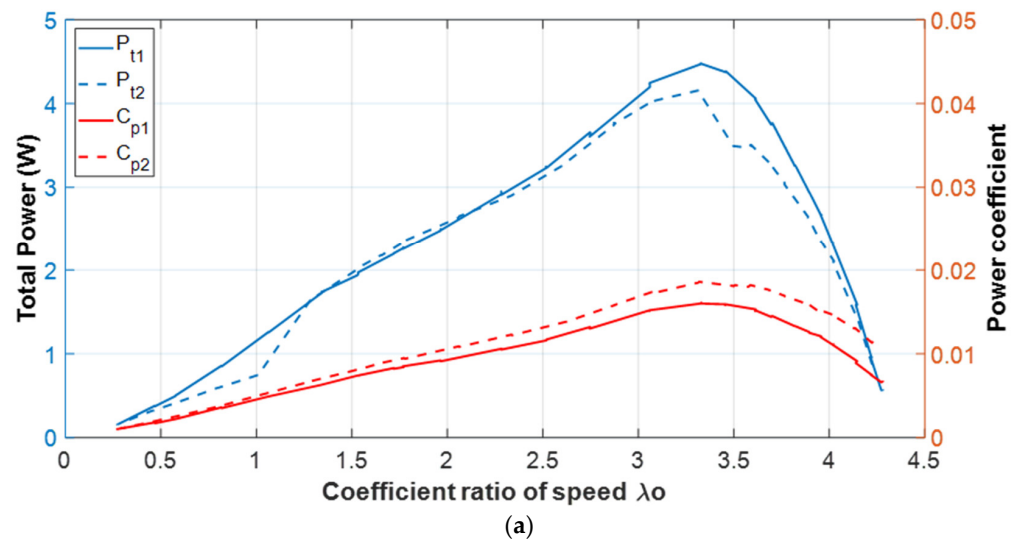


Figure 27. The total power obtained with the symmetrical load case and the asymmetrical load case in the case of wind speeds of 12 m/s (a) and 15 m/s (b).

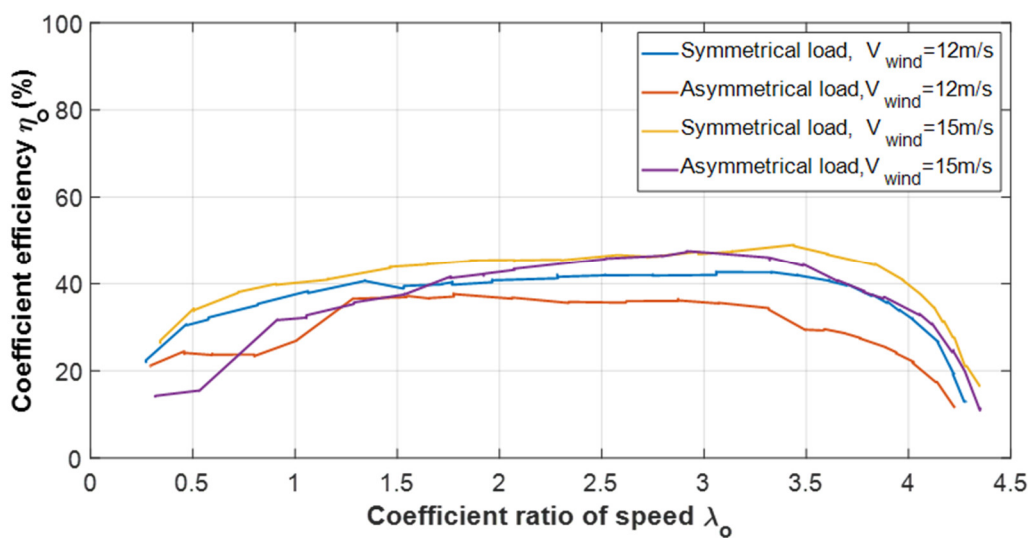
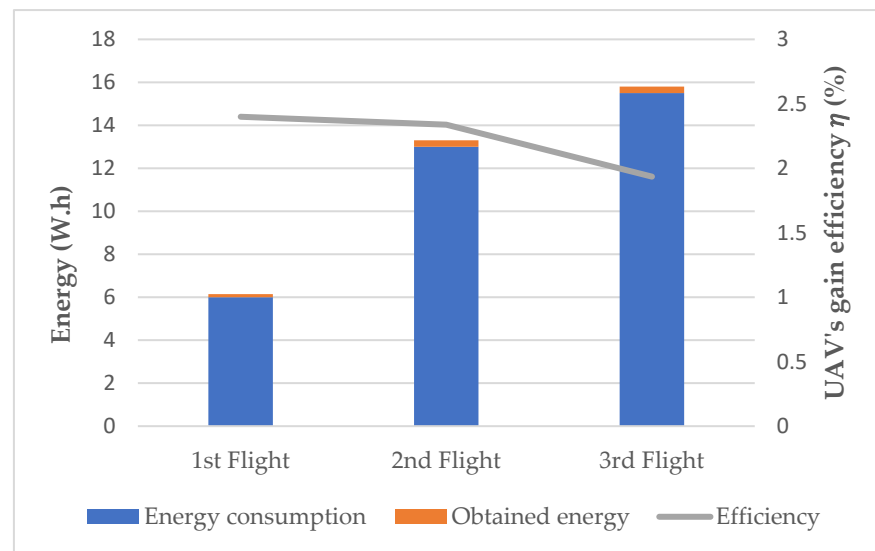


Figure 28. Comparison of the symmetrical and asymmetrical load of a three-phase generator.

In Figure 29, it can be easily noticed that the energy consumed by the UAV during takeoff and flight was very large. However, with the conversion of wind energy to electric energy, the UAV increased its efficiency by approximately 2%. Although this efficiency is limited, optimizing the flight trajectory can increase the conversion rate of wind energy to electrical energy more efficiently.



**Figure 29.** Energy consumption, energy conversion, and gain efficiency of the UAV.

## 5. Conclusions

This paper has contributed to giving an overview of the structure, classification, dynamic model, and control methods of UAVs and one of the current leading concerns about the problem of energy supply for UAV operation. In this paper, two experiments were conducted to evaluate the energy consumption of UAVs and the efficiency of energy conversion from wind energy to electric energy and evaluate the influence of converted energy on the UAV performance. From the results of the first experiment, it was shown that the main energy consumption of the quadrotor was during flight. The energy consumption for the quadrotor to rise to a certain height was quite small compared with the energy that UAV consumed for movement. Therefore, to increase UAV performance, UAVs must fly to high altitudes to take advantage of wind energy, and the energy obtained when converting from wind energy will be suitable in the flight scenario (shown in Figure 3). In the second experiment, the efficiency of energy conversion from wind energy to electric energy was approximately 50%. From there, the UAV's gain efficiency can be calculated. Although, in the experiment, the efficiency of the UAV increased by only approximately 2%, the trajectory planning for the UAV had a great influence on this efficiency. In the future, the authors will conduct other experiments to evaluate the dependence of trajectory planning on the UAV's endurance by using various flight scenarios.

**Author Contributions:** Conceptualization, K.L.P. and J.L.; methodology, K.L.P. and J.L.; software, K.L.P. and N.N.P.; validation, K.L.P. and J.L.; formal analysis, J.L.; investigation, K.L.P., R.B. and J.L.; data curation, K.L.P.; writing—original draft preparation, K.L.P., M.A. and J.L.; writing—review and editing, R.B. and J.L.; visualization, V.T.P. and J.L.; supervision, J.L.; project administration, J.L. All authors have read and agreed to the published version of the manuscript.

**Funding:** This research received no external funding.

**Institutional Review Board Statement:** Not applicable.

**Informed Consent Statement:** Not applicable.

**Data Availability Statement:** Not applicable.

**Acknowledgments:** This work was supported under the project “SV206/2”. The authors appreciate the anonymous reviewer’s clarifications towards the manuscript production.

**Conflicts of Interest:** The authors declare no conflict of interest.

## References

1. Outay, F.; Mengash, H.A.; Adnan, M. Applications of unmanned aerial vehicle (UAV) in road safety, traffic and highway infrastructure management: Recent advances and challenges. *Transp. Res. Part A Policy Pract.* **2020**, *141*, 116–129. [CrossRef]
2. Unmanned Aerial Vehicle (UAV). Market Size to Reach USD 72,320 Million by 2028 at a CAGR of 14.4%. Available online: <https://www.prnewswire.com/in/news-releases/unmanned-aerial-vehicle-uav-market-size-to-reach-usd-72320-million-by-2028-at-a-cagr-of-14-4-valuation-reports-870953616.html> (accessed on 24 May 2022).
3. Kim, J.; Kim, S.; Ju, C.; Son, H.I. Unmanned Aerial Vehicles in Agriculture: A Review of Perspective of Platform, Control, and Applications. *IEEE Access* **2019**, *7*, 105100–105115. [CrossRef]
4. Maddikunta, P.K.R.; Hakak, S.; Alazab, M.; Bhattacharya, S.; Gadekallu, T.R.; Khan, W.Z.; Pham, Q.-V. Unmanned Aerial Vehicles in Smart Agriculture: Applications, Requirements, and Challenges. *IEEE Sens. J.* **2021**, *21*, 17608–17619. [CrossRef]
5. Gao, J.; Hu, Z.; Bian, K.; Mao, X.; Song, L. AQ360: UAV-Aided Air Quality Monitoring by 360-Degree Aerial Panoramic Images in Urban Areas. *IEEE Internet Things J.* **2020**, *8*, 428–442. [CrossRef]
6. Sawadsitang, S.; Niyato, D.; Tan, P.-S.; Wang, P. Joint Ground and Aerial Package Delivery Services: A Stochastic Optimization Approach. *IEEE Trans. Intell. Transp. Syst.* **2018**, *20*, 2241–2254. [CrossRef]
7. Li, X.; Yang, L. Design and Implementation of UAV Intelligent Aerial Photography System. In Proceedings of the 2012 4th International Conference on Intelligent Human-Machine Systems and Cybernetics, Nanchang, China, 26–27 August 2012; pp. 200–203.
8. Liu, J.; Xu, W.; Guo, B.; Zhou, G.; Zhu, H. Accurate Mapping Method for UAV Photogrammetry without Ground Control Points in the Map Projection Frame. *IEEE Trans. Geosci. Remote Sens.* **2021**, *59*, 9673–9681. [CrossRef]
9. Wang, Y.; Bai, P.; Liang, X.; Wang, W.; Zhang, J.; Fu, Q. Reconnaissance Mission Conducted by UAV Swarms Based on Distributed PSO Path Planning Algorithms. *IEEE Access* **2019**, *7*, 105086–105099. [CrossRef]
10. Cho, J.; Sung, J.; Yoon, J.; Lee, H. Towards Persistent Surveillance and Reconnaissance Using a Connected Swarm of Multiple UAVs. *IEEE Access* **2020**, *8*, 157906–157917. [CrossRef]
11. Duan, H.; Zhao, J.; Deng, Y.; Shi, Y.; Ding, X. Dynamic Discrete Pigeon-Inspired Optimization for Multi-UAV Cooperative Search-Attack Mission Planning. *IEEE Trans. Aerosp. Electron. Syst.* **2020**, *57*, 706–720. [CrossRef]
12. Research Questions Accuracy of Drone Data in Agriculture. Available online: <https://internetofbusiness.com/accuracy-drone-data-agriculture> (accessed on 24 May 2022).
13. Monitoring Air Pollution Using Drones. Available online: <https://dronebelow.com/2018/09/13/monitoring-air-pollution-using-drones/> (accessed on 24 May 2022).
14. How Drones (Not the Announcer Kind) Are Improving Sports Coverage. Available online: <https://www.phase1vision.com/blog/drones-in-sports> (accessed on 24 May 2022).
15. Industry Leading VTOL Mapping UAV. Available online: <https://www.deltaquad.com/vtol-drones/map> (accessed on 24 May 2022).
16. Việt Nam “phủ quét” Biển Đông bằng phi đội máy bay không người lái. Available online: <https://soha.vn/viet-nam-phu-quet-bien-dong-bang-phi-doi-may-bay-khong-nguoi-lai-20160606172426413.htm> (accessed on 24 May 2022).
17. Drones Deployed for Maritime Surveillance off France. Available online: <https://www.marinelink.com/news/drones-deployed-maritime-surveillance-off-482264> (accessed on 24 May 2022).
18. What Role and Rules for Canada’s Armed Drones? Available online: [https://www.cgai.ca/what\\_role\\_and\\_rules\\_for\\_canadas\\_armed\\_drones](https://www.cgai.ca/what_role_and_rules_for_canadas_armed_drones) (accessed on 24 May 2022).
19. Aero Surveillance & Lacroix Working on a VTOL UAV-Based Decoy System for Surface Vessels. Available online: <https://www.navyrecognition.com/index.php/naval-news/naval-news-archive/year-2015-news/november-2015-navy-naval-forces-defense-industry-technology-maritime-security-global-news/3253-aero-surveillance-a-lacroix-working-on-a-vtol-uav-based-decoy-system-for-surface-vessels.html> (accessed on 24 May 2022).
20. Li, J.; Zhang, M.; Tay, C.M.J.; Liu, N.; Cui, Y.; Chew, S.C.; Khoo, B.C. Low-Reynolds-number airfoil design optimization using deep-learning-based tailored airfoil modes. *Aerosp. Sci. Technol.* **2021**, *121*, 107309. [CrossRef]
21. Proença, T.; Afonso, F.; Lau, F.; Policarpo, H.; Lourenço, J. On the design and manufacturing of topologically optimized wings. *Rapid Prototyp. J.* **2022**, *28*, 637–646. [CrossRef]
22. Li, H.; Zhang, Y.; Chen, H. Optimization design of airfoils under atmospheric icing conditions for UAV. *Chin. J. Aeronaut.* **2021**, *35*, 118–133. [CrossRef]
23. Jawad, A.M.; Jawad, H.M.; Nordin, R.; Gharghan, S.K.; Abdullah, N.F.; Abu-Alshaeer, M.J. Wireless Power Transfer with Magnetic Resonator Coupling and Sleep/Active Strategy for a Drone Charging Station in Smart Agriculture. *IEEE Access* **2019**, *7*, 139839–139851. [CrossRef]
24. Jaafar, W.; Yanikomeroglu, H. Dynamics of Laser-Charged UAVs: A Battery Perspective. *IEEE Internet Things J.* **2021**, *8*, 10573–10582. [CrossRef]

25. Leuchter, J.; Zobaa, A. Batteries investigations of small Unmanned Aircraft Vehicles. In Proceedings of the 8th IET International Conference on Power Electronics, Machines and Drives (PEMD 2016), Glasgow, UK, 19–21 April 2016; pp. 1–6.
26. Shakhathreh, H.; Sawalmeh, A.H.; Al-Fuqaha, A.; Dou, Z.; Almaita, E.; Khalil, I.; Othman, N.S.; Khreishah, A.; Guizani, M. Unmanned Aerial Vehicles (UAVs): A Survey on Civil Applications and Key Research Challenges. *IEEE Access* **2019**, *7*, 48572–48634. [[CrossRef](#)]
27. Abdelmaksoud, S.I.; Mailah, M.; Abdallah, A.M. Control Strategies and Novel Techniques for Autonomous Rotorcraft Unmanned Aerial Vehicles: A Review. *IEEE Access* **2020**, *8*, 195142–195169. [[CrossRef](#)]
28. Rango, A.; Andrea, L.; Jeffrey, H.; Craig, W.; Kris, H.; Caiti, S.; Dawn, B. Unmanned aerial vehicle-based remote sensing for rangeland assessment, monitoring, and management. *J. Appl. Remote Sens.* **2009**, *3*, 033542.
29. Stewart, M.; Martin, S. Unmanned aerial vehicles: Fundamentals, components, mechanics, and regulations. In *Unmanned Aerial Vehicles*; Nova Science Publishers: Hauppauge, NY, USA, 2020.
30. Austin, R. Introduction to Unmanned Aircraft Systems (UAS). In *Unmanned Aircraft Systems: UAVS Design, Development and Deployment*, 1st ed.; Ian, M., Alan, S., Roy, L., Eds.; Wiley: Hoboken, NJ, USA, 2010.
31. Leuchter, J.; Bajer, J.; Bojda, P. Immunity testing in airborne radio-communication system. In Proceedings of the 2015 IEEE/AIAA 34th Digital Avionics Systems Conference (DASC), Prague, Czech Republic, 13–17 September 2015.
32. Wheeler, P.; Sirimanna, T.S.; Bozhko, S.; Haran, K.S. Electric/Hybrid-Electric Aircraft Propulsion Systems. *Proc. IEEE* **2021**, *109*, 1115–1127. [[CrossRef](#)]
33. Benzaquen, J.; He, J.; Mirafzal, B. Toward more electric powertrains in aircraft: Technical challenges and advancements. *CES Trans. Electr. Mach. Syst.* **2021**, *5*, 177–193. [[CrossRef](#)]
34. Cinar, G.; Markov, A.A.; Gladin, J.C.; Garcia, E.; Mavris, D.N.; Patnaik, S.S. Feasibility Assessments of a Hybrid Turboelectric Medium Altitude Long Endurance Unmanned Aerial Vehicle. In Proceedings of the 2020 AIAA/IEEE Electric Aircraft Technologies Symposium (EATS), Virtual Event, 24–28 August 2020; pp. 1–17.
35. Ye, X.; Al, S.; Antonios, T.; Dan, Z.; Jason, G. Review of hybrid electric powered aircraft, its conceptual design and energy management methodologies. *Chin. J. Aeronaut.* **2021**, *34*, 432–450.
36. Russo, A.; Cavallo, A. Supercapacitor stability and control for More Electric Aircraft application. In Proceedings of the 2020 European Control Conference (ECC), St. Petersburg, Russia, 12–15 May 2020; pp. 1909–1914.
37. Canciello, G.; Russo, A.; Guida, B.; Cavallo, A. Supervisory Control for Energy Storage System Onboard Aircraft. In Proceedings of the 2018 IEEE International Conference on Environment and Electrical Engineering and 2018 IEEE Industrial and Commercial Power Systems Europe (EEEIC/I&CPS Europe), Palermo, Italy, 12–15 June 2018; pp. 1–6.
38. Bolam, R.C.; Vagapov, Y.; Anuchin, A. Review of Electrically Powered Propulsion for Aircraft. In Proceedings of the 53rd International Universities Power Engineering Conference (UPEC), Glasgow, UK, 4–7 September 2018; pp. 1–6.
39. Past Projects: Pathfinder/Pathfinder Plus Solar-Powered Aircraft. Available online: <https://www.nasa.gov/centers/dryden/history/pastprojects/Erast/pathfinder.html> (accessed on 24 May 2022).
40. Dryden Flight Research Center. Available online: <https://www.nasa.gov/centers/dryden/news/ResearchUpdate/Helios/> (accessed on 24 May 2022).
41. Zephyr, the First Stratospheric UAS of Its Kind. Available online: <https://www.airbus.com/en/products-services/defence/uas/uas-solutions/zephyr> (accessed on 24 May 2022).
42. Noman, F.M.; Alkawsy, G.A.; Abbas, D.; Alkahtani, A.A.; Tiong, S.K.; Ekanayake, J. Comprehensive Review of Wind Energy in Malaysia: Past, Present, and Future Research Trends. *IEEE Access* **2020**, *8*, 124526–124543. [[CrossRef](#)]
43. Deittert, M.; Toomer, C.; Richards, A.G.; Pipe, A.G. Engineless UAV propulsion by dynamic soaring. *J. Guid. Control Dyn.* **2009**, *32*, 1446–1457. [[CrossRef](#)]
44. Wei, X.; Yao, P.; Xie, Z. Comprehensive Optimization of Energy Storage and Standoff Tracking for Solar-Powered UAV. *IEEE Syst. J.* **2020**, *14*, 5133–5143. [[CrossRef](#)]
45. Achtelik, M.C.; Stumpf, J.; Gurdan, D.; Doth, K. Design of a flexible high performance quadcopter platform breaking the MAV endurance record with laser power beaming. In Proceedings of the IEEE/RSJ International Conference on Intelligent Robots and Systems, San Francisco, CA, USA, 25–30 September 2011.
46. Yater, J.A.; Lowe, R.A.; Jenkins, P.P.; Landis, G.A. Pulsed laser illumination of photovoltaic cells. In Proceedings of the IEEE 1st World Conference on Photovoltaic Energy Conversion—WCPEC (A Joint Conference of PVSC, PVSEC and PSEC), Waikoloa, HI, USA, 5–9 December 1994.
47. Landis, G.A. Photovoltaic receivers for laser beamed power in space. *J. Propuls. Power* **1993**, *9*, 105–112. [[CrossRef](#)]
48. Wu, J.; Wang, H.; Huang, Y.; Su, Z.; Zhang, M. Energy Management Strategy for Solar-Powered UAV Long-Endurance Target Tracking. *IEEE Trans. Aerosp. Electron. Syst.* **2018**, *55*, 1878–1891. [[CrossRef](#)]
49. Chang, T.; Yu, H. Improving Electric Powered UAVs’ Endurance by Incorporating Battery Dumping Concept. *Procedia Eng.* **2015**, *99*, 168–179. [[CrossRef](#)]
50. Lee, D.; Zhou, J.; Lin, W.T. Autonomous battery swapping system for quadcopter. In Proceedings of the 2015 International Conference on Unmanned Aircraft Systems (ICUAS), Denver, CO, USA, 9–12 June 2015.
51. Lu, M.; Bagheri, M.; James, A.P.; Phung, T. Wireless Charging Techniques for UAVs: A Review, Reconceptualization, and Extension. *IEEE Access* **2018**, *6*, 29865–29884. [[CrossRef](#)]

52. Chittoor, P.K.; Chokkalingam, B.; Mihet-Popa, L. A Review on UAV Wireless Charging: Fundamentals, Applications, Charging Techniques and Standards. *IEEE Access* **2021**, *9*, 69235–69266. [[CrossRef](#)]
53. Zhang, X.; Wang, Y.; Zhu, G.; Chen, X.; Li, Z.; Wang, C.; Su, C.-Y. Compound Adaptive Fuzzy Quantized Control for Quadrotor and Its Experimental Verification. *IEEE Trans. Cybern.* **2021**, *51*, 1121–1133. [[CrossRef](#)]
54. Xi, L.; Wang, X.; Jiao, L.; Lai, S.; Peng, Z.; Chen, B.M. GTO-MPC-Based Target Chasing Using a Quadrotor in Cluttered Environments. *IEEE Trans. Ind. Electron.* **2022**, *69*, 6026–6035. [[CrossRef](#)]
55. Nan, F.; Sun, S.; Foehn, P.; Scaramuzza, D. Nonlinear MPC for Quadrotor Fault-Tolerant Control. *IEEE Robot. Autom. Lett.* **2022**, *7*, 5047–5054. [[CrossRef](#)]
56. McLean, D. Drag and propulsion. In *Understanding Aerodynamics: Arguing from the Real Physics, Aerospace Series*; Wiley: Hoboken, NJ, USA, 2013.
57. Cutler, M. Design and Control of an Autonomous Variable-Pitch Quadrotor Helicopter. Master's Thesis, Massachusetts Institute of Technology, Cambridge, MA, USA, 23 August 2012.
58. Pham, K.L.; Leuchter, J.; Pham, N.N.; Pham, V.T. Design of Commercial-Off-The-Shelf System for Monitoring UAV's Accumulator. In Proceedings of the International Conference on Military Technologies (ICMT), Brno, Czech Republic, 8–11 June 2021; pp. 1–7.